

1 **Geospatial modelling of large wood supply to rivers: a state-of-the-**
2 **art model comparison in Swiss mountain river catchments**

3
4 Nicolas Steeb^{1,*}, Virginia Ruiz-Villanueva^{2,3}, Alexandre Badoux¹, Christian Rickli¹, Andrea
5 Mini³, Markus Stoffel^{2,4,5}, Dieter Rickenmann¹

6
7 ¹Swiss Federal Research Institute WSL, Zürcherstrasse 111, CH-8903 Birmensdorf,
8 Switzerland

9 ²C-CIA-Climate Change Impacts and Risks in the Anthropocene, Institute for Environmental
10 Sciences (ISE), University of Geneva, CH-1205 Geneva, Switzerland

11 ³Institute of Earth Surface Dynamics (IDYST), University of Lausanne, UNIL Mouline, CH-
12 1015 Lausanne, Switzerland

13 ⁴Dendrolab.ch, Department of Earth Sciences, University of Geneva, Geneva, Switzerland.

14 ⁵Department F.-A. Forel for Environmental and Aquatic Sciences, University of Geneva,
15 Geneva, Switzerland

16 *Corresponding author: Nicolas Steeb, Email: nicolas.steeb@wsl.ch

17

18 **ABSTRACT**

19 Different models have been used in science and practice to identify instream large wood
20 (LW) sources and to estimate LW supply to rivers. This contribution reviews the existing models
21 proposed in the last 35 years and compares two of the most recent GIS-based models by applying
22 them to 40 catchments in Switzerland. Both models, which we call here empirical GIS approach
23 (EGA) and Fuzzy-Logic GIS approach (FGA), consider landslides, debris flows, bank erosion,
24 and mobilization of instream wood as recruitment processes and compute volumetric estimates
25 of LW supply based on three different scenarios of process frequency and magnitude. Despite
26 being developed following similar concepts and fed with similar input data, the results from the
27 two models differ markedly. In general, estimated supply wood volumes were larger in each of
28 the scenarios when computed with the FGA and lower with the EGA models. Landslides were
29 the dominant process identified by the EGA, whereas bank erosion was the predominant process
30 according to the FGA model. These differences are discussed, and results are compared to
31 available observations coming from a unique database. Regardless of the limitations of these
32 models, they are useful tools~~proved extremely useful~~ for hazard assessment, ~~and~~ the design of
33 infrastructure, and other management strategies.

34
35 **KEYWORDS:** large wood, GIS, modelling, landslide, bank erosion, debris flow, natural
36 hazards

37

38 1 INTRODUCTION

39 The influence of wood in watercourses is manifold. On the one hand, there are various
40 ecological benefits of large wood (LW), as it provides habitats and a food source for many organic
41 organisms, thus promoting rich biodiversity (Harmon et al., 2004; Steel et al., 2003; Wondzell
42 and Bisson, 2003). LW also affects stream hydraulics by altering the channel morphology and
43 sediment control (Montgomery and Piégay, 2003; Wohl and Scott, 2016). On the other hand, large
44 quantities of LW may be mobilized during infrequent, high-magnitude floods and may induce
45 potential hazards for human settlements and infrastructure (Lucía et al., 2015c; Lucía et al., 2018;
46 Rickli et al., 2018; Ruiz-Villanueva et al., 2013; Steeb et al., 2017b). Consequently, river
47 managers are challenged to maintain a good ecological status of rivers while minimizing potential
48 hazards.

49 From a flood protection perspective, the main problem regarding LW in streams is wood
50 accumulation at bridges, and weirs, which reduces or even clogs the entire river cross section and
51 leads to backwater rise and consequent inundation (Comiti et al., 2016; Lassetre and Kondolf,
52 2012; Piégay et al., 1999; Rickenmann et al., 2016). The associated damage potential of LW may
53 depend, among other variables, ~~s~~ mainly on the volume of transported LW (Mazzorana et al.,
54 2018). Large wood transport is governed by the flow conditions, river morphology (Ruiz-
55 Villanueva et al., 2020), the size and shape of individual wood pieces (i.e., large logs or rootwads
56 are more prone to clogging; Bezzola et al., 2002), the mode wood is being transported (i.e., if logs
57 are transported congested or not; Braudrick et al., 1997; Ruiz-Villanueva et al., 2019) and the
58 availability or supply of wood. Wood supply occurs by numerous geomorphic processes including
59 bank erosion, channel migration, mass wasting (e.g., landslides, debris flows) and natural tree
60 mortality and fall (Benda and Sias, 2003). These processes can be highly variable, both on
61 temporal and spatial scales (Gasser et al., 2019).

62 Despite numerous existing approaches and efforts (see following section), the quantitative
63 estimation of LW supply volume and the definition of contributing source areas based on different
64 recruitment processes remain very challenging. [The estimation of exported wood involves many](#)

65 uncertainties that are difficult to quantify, because LW transport happens at the end of a long
66 process cascade, usually starting with precipitation as a trigger, followed by a flood formation
67 and the occurrence of recruitment processes as wood suppliers, and the increased discharge as a
68 transport medium.~~Because LW transport happens at the end of a long process cascade~~
69 ~~(precipitation as trigger, flood formation and recruitment processes as supplier, channel discharge~~
70 ~~as transport medium), its estimation involves many uncertainties that are difficult to quantify.~~ In
71 addition, any type of model developed to estimate and quantify wood supply should be validated
72 with field observations, data that is very scarce (Comiti et al., 2016; Nakamura et al., 2017; Wohl
73 et al., 2019; Gurnell & Bertoldi, 2020).

74 This work reviews the state-of-the-art in wood supply modelling and presents a comparison
75 of two recent GIS-based approaches that were developed in the context of an applied research
76 project funded by the Swiss Federal Office for the Environment. First, the literature review
77 provides an updated compilation of published approaches to model recruitment processes to
78 quantify LW supply, classifying the approaches by model type and summarizing their main
79 characteristics, such as processes considered, and their temporal and spatial scales. We then focus
80 on two GIS-based models that were developed based on a similar general concept, used similar
81 input data and were applied to the same study sites. The models were validated with a unique
82 observation dataset of supplied wood during single events in a large number of catchments in
83 Switzerland (Steeb, 2018; Steeb et al., 2019a). Despite their similarities, the models differ in some
84 respects and result in somewhat different outcomes. These differences are used to stress the
85 limitations and strengths of the two models, to compare them with other recent approaches
86 included in the literature review and to discuss uncertainties and challenges related to the
87 modelling of LW supply. In addition, we also consider implications for flood hazard assessment
88 and river management.

89 ~~This work reviews the state-of-the-art in wood supply modelling and presents a comparison~~
90 ~~of two recent GIS-based approaches based on a similar general concept and using similar input~~
91 ~~data. The models were validated with a unique observation dataset of supplied wood during single~~

92 ~~events in a large number of catchments in Switzerland (Steeb, 2018; Steeb et al., 2019a). We~~
93 ~~discuss uncertainties, limitations and strengths of the two models and compare them with other~~
94 ~~recent approaches. In addition, we also consider implications for flood hazard assessment and~~
95 ~~river management.~~

96

97 **2 LARGE WOOD SUPPLY MODELS: A REVIEW**

98 Over the last decades, different approaches have been developed to quantify LW supply at
99 both, reach and catchment scales. Gregory et al. (2003) provided a summary of the first attempts
100 to simulate wood supply, i.e., mostly mathematical models developed from conceptual
101 descriptions of selected wood recruitment processes. Later, Gasser et al. (2019) reviewed recent
102 approaches and evaluated whether the stabilizing effect of vegetation on total LW supply was
103 considered or not. ~~Here~~ In this work, we compile ~~information on existing approaches~~ and expand
104 these previous overviews to provide an updated review of published approaches to model
105 recruitment processes and to quantify LW supply (

106 **Table 1; numbering therein used for reference in this section).** We classify the approaches by
107 model category (i.e., empirical, deterministic, stochastic, or GIS-based) and summarize their main
108 characteristics (i.e., processes considered, spatial and temporal scales, inputs and outputs, and
109 whether they were validated with field observations or not). The evolution of these models
110 illustrates and contributes to the scientific understanding of the complex processes involved in
111 wood supply to rivers. Some of the earliest approaches, [e.g., \[1\], \[21\], \[22\]](#), ~~(e.g., Malanson and~~
112 ~~Kupfer, 1993; also Minor, 1997); Rainville et al., 1986; Van Sickle and Gregory, 1990)~~ were
113 designed to simulate long-term delivery of wood to river reaches from adjacent riparian forest by
114 tree mortality, windthrow or bank erosion. Subsequent models attempted to describe these input
115 processes over larger portions of river networks [3], [4], [6], [23], [24] ~~(Beechie et al., 2000;~~
116 ~~Bragg, 2000; Downs and Simon, 2001; Kennard et al., 1999; Meleason et al., 2003; Welty et al.,~~
117 ~~2002)~~, but maintained a long-term perspective. Few studies included other processes, such as
118 channel avulsion [4], [22] ~~(Malanson and Kupfer, 1993; Downs and Simon, 2001)~~. These earlier
119 models were developed in the US, most of them in the Pacific Northwest and a few in the
120 Southeast [4] ~~(e.g., Downs and Simon, 2001)~~ or the Rocky Mountains ~~(e.g., Bragg, 2000)~~ [23].
121 Later, researchers started to apply and develop models elsewhere, ~~e.g., in~~ New Zealand [24];
122 ~~Meleason et al., 2003)~~.

123 Martin and Benda (2001) and Benda and Sias (2003) [16] were pioneers in considering mass
124 movements (i.e., landslides and debris flows) as wood recruitment processes, and they established
125 the first conceptual framework for LW budgeting. This approach has been further applied in US
126 mountain rivers [8], [20] ~~(Benda and Bigelow, 2014; Hassan et al., 2016)~~ before it has been
127 adapted to shorter timescales for mountain rivers in Italy and Switzerland [14], [29] ~~(also Comiti~~
128 ~~et al., 2016; Lucía et al., 2018; Steeb et al., 2017b)~~. Focusing on shorter time windows and on
129 episodic disturbances (e.g., floods) aggregated at the catchment scale, researchers proposed
130 empirical equations based on field observations of exported wood and catchment characteristics
131 [28], [29]

132 ~~(Rickenmann, 1997; also Rimböck, 2003; Steeb, 2018; Steeb et al., 2019a; Uchiogi et al.,~~
133 ~~1996)~~. As most of the data used to derive such empirical formulas originated from steep headwater
134 streams and mountain rivers in Switzerland, Austria, and Japan, application to larger catchments
135 is associated with considerable uncertainty.

136 The rapid proliferation of remote sensing and the advances in computing sciences and
137 geographic information systems (GIS; Bishop and Giardino, 2022) resulted in the development
138 of another group of models (i.e., geospatial models). These GIS-based models allow a spatially
139 explicit assessment of different LW recruitment processes, the identification of source areas and
140 the estimation of LW volumes, expanding the analysis to larger areas, covering multiple (sub-
141)catchments.~~In order to extend the analysis to larger areas, covering multiple (sub-)catchments~~
142 ~~and applying a spatially distributed analysis, another group of models (i.e., geospatial models)~~
143 ~~used geographic information systems (GIS) that allowed a spatially explicit assessment of~~
144 ~~different LW recruitment processes, the identification of source areas and the estimation of LW~~
145 ~~volumes.~~ Rimböck (2001) [5] developed a GIS-based model to identify potential recruitment
146 areas of LW in mountain streams, resulting from bank erosion, landslides and windthrow. In this
147 approach, he used wood volume reduction factors to distinguish between the potential LW volume
148 (i.e., maximum volume that could potentially be supplied) and the estimated wood volume
149 exported or supplied during exceptional floods. Mazzorana et al. (2009) [10] developed a
150 procedure to determine the relative propensity of mountain streams in Bolzano Province (Italy)
151 to supply wood due to floods, debris flows in tributaries, bank erosion and shallow landslides,
152 based on empirical indicators. Kasprak et al. (2012) [18] used light detection and ranging
153 (LiDAR) data to estimate tree height and recruitable tree abundance throughout a watershed in
154 US Coastal Maine, and to determine the likelihood for the stream to recruit channel-spanning
155 trees at the reach scale and assess whether mass wasting or channel migration was a dominant
156 supply mechanism. Ruiz-Villanueva et al. (2014c) [12] estimated potential LW volumes recruited
157 from landslides, bank erosion and fluvial transport during floods in the Central Mountain Range
158 in Spain. The authors applied a GIS model including multi-criteria and multi-objective

159 assessments using fuzzy logic principles together with reduction factors for predefined scenarios.
160 The method included the analysis of the hillslope-channel network connectivity and the resistance
161 of the vegetation to be eroded. This approach was recently adapted and applied to mountain
162 catchments in Switzerland, considering debris flows as supply processes as well [13] ~~(Ruiz-~~
163 ~~Villanueva and Stoffel, 2018)~~, and it has been further used in the present study. Also applied in
164 Swiss mountain catchments, Steeb et al. (2017a, 2019b) [11] proposed a GIS approach to model
165 source areas of LW and to estimate potential supply and exported wood volumes based on
166 reduction factors derived from an extensive empirical database of flood events with LW
167 occurrence (Steeb, 2018; Steeb et al., 2019a, 2022). In Switzerland and other countries around
168 the Alps, some private engineering companies and consultants, specialized on natural hazards,
169 developed their own GIS-based models to estimate the potential LW supply from different
170 recruitment processes (e.g., von Glutz, 2011; Hunziker, 2017).

171 However, one important aspect of the above-mentioned GIS-based models [10], [5], [12],
172 [11] ~~(Mazzorana et al., 2009; Rimböck, 2001; Ruiz Villanueva et al., 2014c; Steeb et al., 2017a,~~
173 ~~2019b)~~ is that they do not attempt to simulate the actual recruitment processes (e.g., landslides,
174 debris flows, bank erosion), but they used available information on areas susceptible to
175 recruitment processes (e.g., from hazard maps, although these are usually derived from previous
176 modelling studies) or expert-based buffers. An intermediate approach was proposed by Rigon et
177 al. (2012) [19], who applied a geostatistical bivariate analysis (weight of evidence method;
178 Bonham-Carter et al., 1990) to identify unstable areas based on weighting factors. Lucía et al.
179 (2015a) [14] estimated potential LW recruitment in a mountain basin in Italy modelling shallow
180 landslides with a hillslope stability model (Montgomery and Dietrich, 1994) coupled to a
181 connectivity index (Cavalli et al., 2013). The approach was further developed by Franceschi et al.
182 (2019) [15] who used detailed forest information based on a single tree extraction from LiDAR
183 data and combined it with a 1D hydraulic model to evaluate channel widening and LW
184 downstream propagation. Cislighi et al. (2018) [27] proposed one of the first physically-based
185 stochastic models to simulate shallow landslides combined with the forest stand characteristics to

186 estimate LW recruitment from hillslopes. Similarly, Gasser et al. (2018, 2020) [26] proposed two
187 frameworks to model shallow landslides, and geotechnical and hydraulic bank erosion applying
188 two physically-based stochastic models together with a tree detection algorithm (Dorren, 2017)
189 to estimate LW supply. Zischg et al. (2018) [9] presented a LW recruitment model coupled to a
190 2D hydrodynamic model to estimate LW recruitment from bank erosion in the flood influence
191 zone of the river. In this approach, wood volumes were also estimated based on a single tree
192 detection algorithm applied to a normalized digital surface model.

Spatial scale	Reference	Country	Model name	Processes considered	Temporal scale	Main input variables	Output
Deterministic models							
Stream reach	[1] Rainville et al., 1986	USA (Pacific Northwest)	Not specified	Tree fall	between 25 and 300 years (time steps of 10 years)	Not specified	Number of wood pieces
	[2] Murphy and Koski, 1989	SE Alaska	Not specified	Tree fall and bank erosion	250 years (time steps 1 year)	Survey measurements; channel width, wood diameter, forest stand	Number of wood pieces
	[3] Beechie et al., 2000 (based on Kennard et al., 1999)	USA (WA)	Riparian-in-a-Box	Natural tree mortality, windthrow, bank erosion	150 years (time steps 10 years)	Tree species, diameter, height, and crown ratio in stands; site/reach geometry	Number of wood pieces and LW volume
	[4] Downs and Simon, 2001 (based on earlier models of Simon, 1989 and Hupp and Simon, 1991)	USA (MS)	Simon channel evolution model	Bank erosion and channel avulsion	time steps of 10 years	Channel morphology surveys, rates of knickpoint migration, quantitative characteristics of riparian vegetation	Number of wood pieces and LW volume
	[5] Rimböck, 2001	Germany (Bavarian Alps)	<i>Luftbildbasierte Abschätzung des Schwemmholtzpotenzials LASP</i> (aerial photo-based estimation of wood potential volume)	Bank erosion, mass failures (i.e., landslides), windthrow, avalanches	Event	DTM, stand density	LW potential volume
	[6] Welty et al., 2002 (same as Kennard et al., 1999 and Beechie et al., 2000)	USA (Pacific Northwest)	Riparian aquatic interaction simulator RAIS	Natural tree mortality, windthrow, bank erosion, mass failures	240 years (time steps 10 years)	Various variables describing forest stand, stream width, initial LW, conifer/hardwood depletion rate, zone widths, windthrow rate, fall direction bias, LW placement option	Number of wood pieces and LW volume
	[7] Benda et al., 2016 (sensu Benda and Sias 2003)	USA (OR)	Reach Scale Wood Model (RSWM)	Tree fall by natural mortality	100 years (5-year time steps)	Stand density, mortality rate, tree height & diameter, slope, stream width	Number of wood pieces and LW volume
	[8] Hassan et al., 2016 (budget concept used in Benda and Sias 2003)	Canada (BC)	Not specified	Tree mortality, bank erosion, mass failures	100 years period	High field data requirements, most can be obtained from air photo measurements, forest inventory data, and/or regional values	LW volume
	[9] Zischg et al., 2018	Switzerland	LWDsimR (coupled with Basement-ETH)	Bank erosion	Event	DEM, hydrograph, forest stand	LW volume
	Catchment	[10] Mazzorana et al., 2009	Italy (Autonomous Province of Bolzano)	Not specified	Bank erosion, mass failures, and debris flows	Event	DTM, hazard index map (debris flow, overbank sedimentation), land use map, stand map, torrent network map

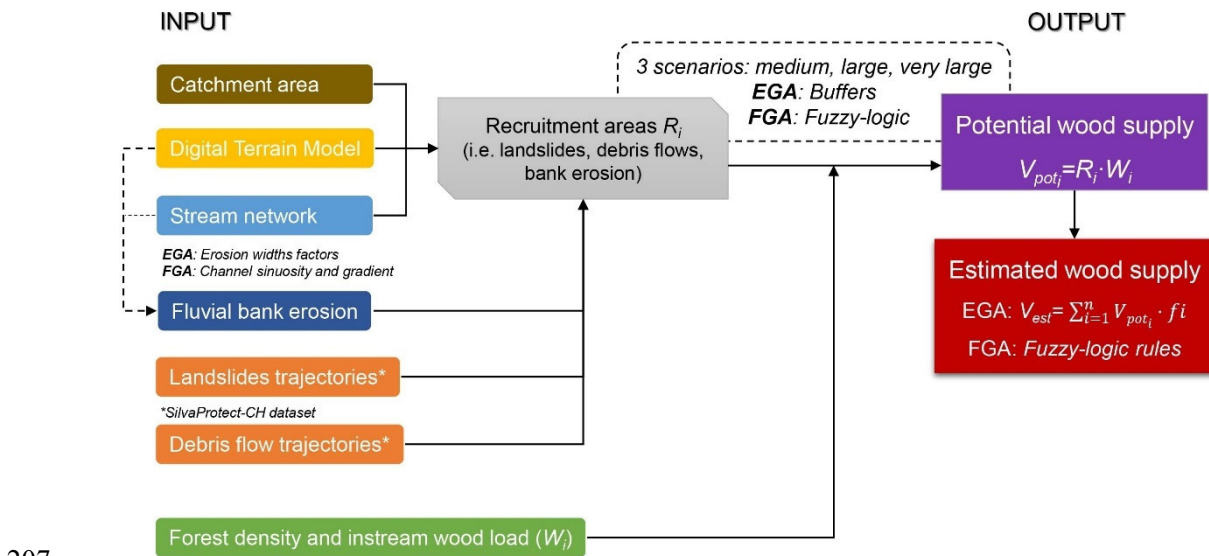
							a propensity to entrain and deliver LW
	[11] Steeb et al., 2017a, 2019b	Switzerland (Alps)	Empirical GIS Approach (EGA)	Bank erosion, mass failures, debris flows	Event	SilvaProtect-CH data, stream network, catchment area, ecomorphology data, stand data (NFI)	Number of wood pieces and LW volume
	[12] Ruiz-Villanueva et al., 2014c	Spain	Not specified	Fluvial transport, bank erosion and mass failures (i.e., landslides)	Event	DEM, topography, natural hazards maps, geomorphological units, forest density, tree species, height & diameter	Number of wood pieces and LW volume
	[13] Ruiz-Villanueva and Stoffel, 2018	Switzerland	Fuzzy-logic GIS Approach (FGA)	Bank erosion, mass failures, debris flows	Event	SilvaProtect-CH data, stream network, catchment area, DEM, ecomorphology data, stand data (NFI)	LW volume
	[14] Lucía et al., 2015a	Italy (North-western Apennines)	Not specified	Bank erosion, mass failures	Event	DTM, DSM (digital surface model)	LW volume
	[15] Franceschi et al., 2019 (based on the model developed by Lucía et al. 2015)	Italy (South Tyrol)	Not specified	Bank erosion, mass failures	Event	DTM, geomorphological map, precipitation, discharge	LW volume
Both stream reach and catchment	[16] Benda and Sias, 2003	USA (Pacific Northwest)	Not specified	Episodic tree mortality (e.g., fire, wind), bank erosion, mass failures, and debris flows	800-1800 years (time steps 10 years)	Stand density, tree height, channel width, recruitment area & rates	Number of wood pieces and LW volume
	[17] Benda et al., 2007	USA	NetMap	Hillslope erosion, sediment, and wood supply	Not specified	Base terrain parameters including DEM and climate data	LW accumulation type
	[18] Kasprak et al., 2012	USA (ME)	Not specified	Bank erosion, mass failures, and debris flows	100 years period	Stand data, LiDAR DEM	Number of wood pieces
	[19] Rigon et al., 2012	Italy (Eastern Alps)	Not specified	Mass failures (i.e., landslides)	Event	Landslide and debris flow inventory data, stand data, DEM	LW volume
	[20] Benda and Bigelow, 2014 (same model as Benda and Sias, 2003)	USA (CA)	Not specified	Tree mortality, bank erosion, mass failures, debris flows and snow avalanches	100 years period	Survey measurements	wood recruitment, storage and transport
Stochastic models							
Stream reach	[21] Van Sickle and Gregory, 1990	USA (OR)	Not specified	Tree fall	time steps of 10 years	Riparian stand density, tree height, stream length	Number of wood pieces
	[22] Malanson and Kupfer, 1993	USA	FORFLO model	Tree fall	500 years (time steps 1 year)	Tree species, tree height, diameter, water level	Biomass
	[23] Bragg, 2000	USA (Inter-mountain West)	CWD model (1.2)	Episodic tree mortality (spruce beetle outbreak, moderately intense fire, and clear-cut)	300 years (time steps 10 years)	Stand density, species, tree height & diameter	Number of wood pieces and LW volume

	[24] Meleason et al., 2003	USA (Pacific Northwest)	Streamwood	Tree fall by natural mortality	500 years (time steps 10 years)	List of trees that died in a year (wood model input = forest model output)	Number of wood pieces and LW volume
	[25] Eaton et al., 2012	British Columbia	The reach-scale channel simulator (RSCS) was	Tree fall by natural mortality	One-year time step	Tree height, tree diameter, tree fall orientation, forest density, chronic mortality, decay and breakage	Wood load ($m^3 \cdot m^{-2}$) and jam formation
	[26] Gasser et al., 2018 and 2020	Switzerland	SlideforMAP, BankforMAP, FINT	Bank erosion, mass failures	Event	DTM, DSM, precipitation maps, soil map, vegetation efficiency (erosion prevention)	LW volume
Catchment	[27] Cislighi et al., 2018	Italy (Eastern Alps)	Probabilistic PRIMULA model and a hillslope-channel transfer mode	Mass failures (i.e., landslides)	Event	DEM, geological map, rainfall, forest stand characteristics	LW volume
Empirical models							
Catchment	[28] Rickenmann, 1997	Switzerland, Japan, USA	Not specified	Wood export, (recruitment process not specified)	Event	Catchment area, forested catchment area, stream length, forested stream length, peak flow, flood runoff, and bedload volume	LW potential (instream wood), estimated LW supply volumes
	[29] Steeb et al., 2017b; Steeb, 2018 (updated from Rickenmann, 1997)	Switzerland, Italy, France, Germany Japan	Not specified	Wood export, (recruitment process not specified)	Event	Catchment characteristics, flood event characteristics	LW volume

196 **3 GEOSPATIAL MODELLING OF LARGE WOOD SUPPLY IN**
 197 **SWISS MOUNTAIN CATCHMENTS**

198 **3.1 General concept**

199 In this contribution, two LW models were compared; the empirical GIS approach (EGA)
 200 by Steeb et al. (2017a, 2019b) and the Fuzzy-Logic GIS approach (FGA) by Ruiz-Villanueva and
 201 Stoffel (2018) which is a variation of the model presented by Ruiz-Villanueva et al. (2014c). Both,
 202 the EGA and FGA are based on a similar general concept (Figure 1) and fed with similar input
 203 data and defined equivalent scenarios (see following subsections) to make comparison possible.
 204 Both models were developed in the context of *WoodFlow*, a Swiss research program aimed at
 205 creating knowledge and methods to [analyze](#) instream wood dynamics, with particular
 206 attention to watercourses in the Alpine region (FOEN, 2019).



207
 208 **Figure 1: Conceptual model of the empirical GIS approach (EGA) and the Fuzzy-Logic GIS**
 209 **approach (FGA). V_{pot} = potential wood supply [m³]; V_{est} = estimated supplied wood [m³];**
 210 **i = recruitment process[-]; R = recruitment area [ha]; W = forest density or instream wood load**
 211 **[m³ ha⁻¹]; f = volume reduction factor [-]. [Three different scenarios were defined \(see section 3.5\):](#)**
 212 **[medium scenario \(medium-to-high frequency and intermediate magnitude\), large scenario \(relatively](#)**
 213 **[low frequency and medium-to-high magnitude\), and very large scenario \(very low frequency and](#)**
 214 **[very high magnitude\).](#)**

215

216 The general concepts and main steps of the GIS-based approaches were to (i) identify the
217 recruitment areas on the hillslopes and along the stream network that may contribute woody
218 material to streams, such as areas affected by landslides, debris flows and bank erosion; (ii) create
219 three different scenarios based on the process frequency and magnitude; and to (iii) provide
220 estimates of potential LW supply V_{pot} (i.e., worst case scenarios) and supplied wood volumes for
221 each scenario V_{est} . The methods aim at estimating supply wood volumes at the catchment scale
222 and do not include the analysis of wood transfer (i.e., transport and deposition) through the stream
223 network.

224 Potential large wood supply V_{pot} was calculated by intersection of the modelled recruitment
225 areas with forest cover. During a flood, however, only a part of the LW potential is actually
226 recruited and exported out of the catchment. Therefore, empirically derived volume reduction
227 factors (EGA) or fuzzy logic principles (FGA) were applied to best estimate actual supplied LW
228 volumes V_{est} . Modelling results were validated by comparison with available empirical data
229 documented after flood events [in Switzerland \(Steeb et al., 2021, 2022\). This dataset documents](#)
230 [recruited and transported quantities of large wood together with the associated catchment and](#)
231 [flood-specific parameters, including the associated recruitment processes](#) (Table S1 in
232 supplementary material).

233

234 **3.2 Input data**

235 *3.2.1 Catchment areas and stream network*

236 The topographical catchment areas (feature polygons), which define the perimeters of
237 investigation, were available from the geodataset “topographical catchments of Swiss
238 waterbodies” (FOEN, 2015). The stream network of Switzerland at a scale of 1:25,000
239 (swissTLM3D, © 2016 swisstopo [DV033594]) was pre-processed by adding information on
240 channel width as derived from a Swiss-wide ecomorphological dataset (Ökomorphologie
241 Stufe F ©FOEN; Zeh Weissmann et al., 2009). Based on this dataset, the channel width was

242 known for 42 % (25,800 km) of the total Swiss streams' length. For the remaining 58 %, we
243 extrapolated channel width based on stream order (Strahler, 1957) and altitude classes (Table S2).

244 The stream network and channel widths were used to define intersections and connectivity
245 between the hillslopes processes and the streams, to estimate the bank erosion prone areas
246 (sections 3.3 and 3.4) and to assign values of instream dead wood volumes (section 3.2.3).

247

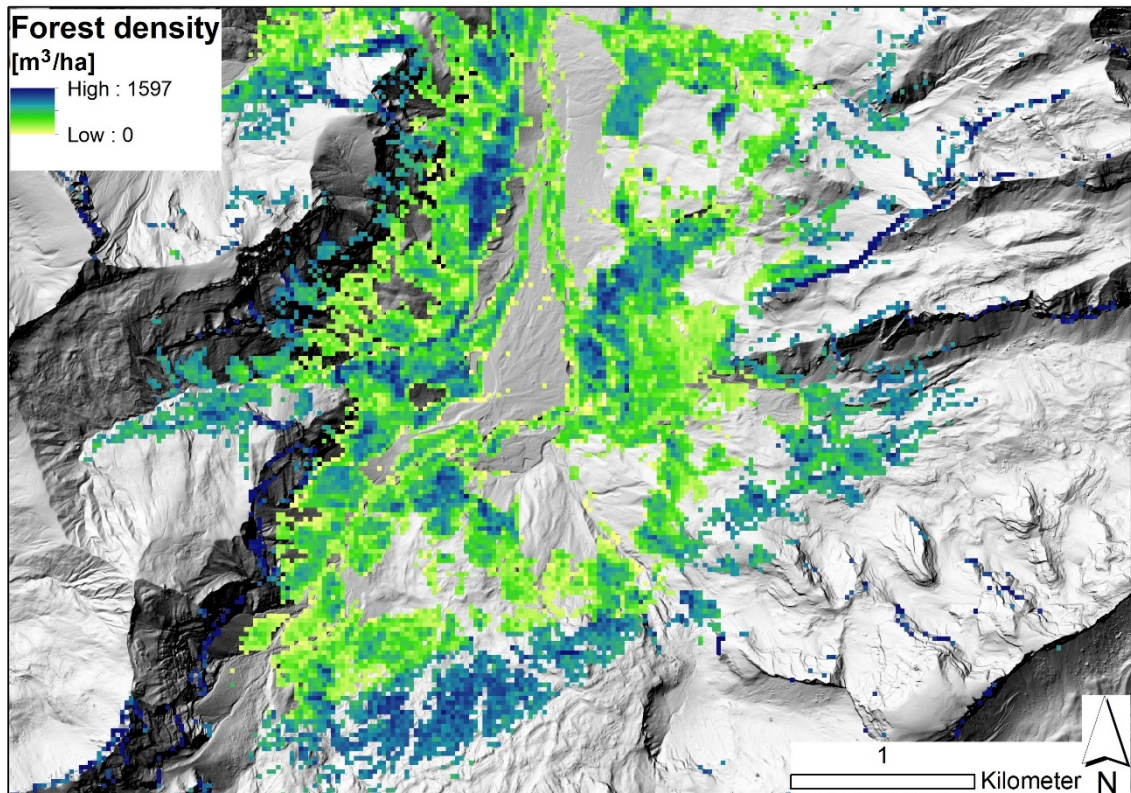
248 *3.2.2 SilvaProtect-CH and the identification of landslide and debris flow* 249 *trajectories*

250 For the modelling of the two recruitment process categories landslide and debris flow, both
251 GIS models used the SilvaProtect-CH dataset from Losey and Wehrli (2013). As part of the
252 SilvaProtect-CH project, several natural hazard processes were modelled over the entire Swiss
253 territory using partly physically-based models. As a result, process trajectories that describe the
254 topographic flow path and runout distances (from starting to deposition zone) of the investigated
255 natural hazard processes were readily available (details are provided in the supplementary
256 material). These trajectories were processed further to identify potential recruitment areas of LW
257 supply (sections 3.3. and 3.4).

258

259 *3.2.3 Forest density and instream wood load*

260 The density of living trees in Swiss forests [$\text{m}^3 \text{ha}^{-1}$] was derived from a Swiss nationwide
261 raster map with an original resolution of 25 x 25 m (rescaled to 1 x 1 m; Figure 2). The raster map
262 is based on a growing stock model developed by Ginzler et al. (2019) that quantifies forest density
263 in relation to tree height (based on airborne stereo imagery), canopy cover, topographic position
264 index, mean summer temperature and elevation. The EGA and FGA models further consider an
265 estimate of deadwood on the forest floor [$\text{m}^3 \text{ha}^{-1}$] (i.e., equal to 5% of living trees density) based
266 on empirical data of the Swiss National Forest Inventory (NFI; WSL, 2016).



267

268

269

270

Figure 2: [Snapshot-Example](#) of the wood stock raster map in the Grosse Melchaa catchment near Stöckalp (Canton Obwalden). Background: Digital terrain model (hillshade), © swisstopo.

271

272

273

274

275

276

277

Additionally, instream wood loads were included in the calculations, accounting for potential LW volumes from accumulated deadwood in the channel. Detailed information on wood loads across the stream network was not available, so based on a literature review by Rickli and Bucher (2006) and Ruiz-Villanueva et al. (2016), volumes of instream wood were assigned to the different streams grouped by channel width (EGA) or by stream order (FGA) classes (see following sections).

278 **3.3 The empirical GIS approach (EGA)**

279 Debris flow and landslide trajectories from SilvaProtect-CH were constrained by
280 intersection with the stream network and forest cover. Only landslide trajectories with starting
281 points within a 50-m distance from the stream network were considered. This limitation was
282 supported by the landslide database of Rickli et al. (2016) where 44 % of all documented
283 landslides showed a runout distance of less than 50 m (around 80 % are within a distance of
284 100 m). For each scenario (section 3.5), different buffer widths w_b were applied on both sides of
285 the relevant debris flow and landslide trajectories (i.e., medium scenario: $w_b = 5$ m; large scenario:
286 $w_b = 10$ m; very large scenario: $w_b = 15$ m). The buffer widths were chosen in ranges according
287 to the Swiss landslide database (Rickli et al., 2016). Potential recruitment areas were finally
288 extracted as the overlap of the buffered trajectories with the forest layer.

289 The extent of bank erosion in EGA was assumed to be proportional to the given channel
290 width. Scenario-specific erosion width factors e_w (i.e., a multiple of the channel width) were
291 empirically derived from observations after the well-documented August 2005 flood in
292 Switzerland, for which a large dataset was analysed and made available (Bachmann Walker, 2012;
293 Hunzinger and Durrer, 2008). Scenario-specific erosion width factors were $e_w = 1.5$ for the
294 medium scenario, $e_w = 3$ for the large scenario, and $e_w = 4.5$ for the very large scenario. The
295 resulting buffer widths were added to the original channel width. Potential recruitment areas due
296 to bank erosion were finally extracted as the overlap of the buffered stream network with the
297 forest layer.

298 The estimation of previously stored wood load within the river network (i.e., instream
299 deadwood) was based on empirical values of wood storage per stream hectare. Rickli et al. (2018)
300 documented instream wood storage for ten reaches in Swiss torrents. This database was
301 complemented with 39 additional values from various other European rivers, based on a literature
302 review by Ruiz-Villanueva et al. (2016), in order to have reliable derivations. Finally, we assigned
303 wood load values into three channel width classes (i.e., <5 m = $94 \text{ m}^3 \cdot \text{ha}^{-1}$; 5-10 m = $67 \text{ m}^3 \cdot \text{ha}^{-1}$;
304 >10 m = $42 \text{ m}^3 \cdot \text{ha}^{-1}$).

305 Potential source areas from different recruitment processes may partly overlap. For this
306 reason, a priority sequence was determined so that such overlapping areas were not counted more
307 than once. This was defined according to the following principle: The closer to the channel a
308 recruitment process occurs, the higher the priority: instream wood > debris flow > bank erosion
309 > landslide. For example, overlapping areas of debris flows and bank erosion were assigned to
310 the process area debris flow.

311 Potential recruitment areas were finally used to calculate the potential LW supply V_{pot} by
312 multiplying the process areas with the respective forest density (for debris flows, landslides and
313 bank erosion) or wood load (for instream deadwood). From the resulting potential LW supply,
314 the actual LW supply V_{est} was estimated. To do so, volume reduction factors f were used, which
315 assumed different values depending on the recruitment process and scenario of process magnitude
316 (Table 2). The volume reduction factors were empirically determined with three different
317 approaches (Steeb et al., 2019b): 1) Comparison with literature data, including values from other
318 studies and models that proposed reduction factors; 2) comparison of potential vs. observed
319 recruitment areas; and 3) comparison of estimated vs. observed wood volumes [from-in well](#)
320 [documented catchments during the 2005 ~~previous~~ floods](#) (see the five blue catchments in Figure
321 3).

322 Values of observed LW supply volumes and recruitment areas together with the associated
323 catchment and flood specific parameters were taken from a complementary empirical dataset that
324 was also part of the WoodFlow research program. In total, the LW database consisted of 210 data
325 entries. Most entries (171) refer to events in Switzerland. Also included are flood events from
326 Japan, Italy, Germany and France (Steeb et al., 2019a).

327

328 **Table 2: Overview of volume reduction factors f , classified by scenario and recruitment**
 329 **processes.**

Scenario	Instream wood	Debris flow	Bank erosion	Landslide
Medium	0.10	0.05	0.05	0.01
Large	0.30	0.10	0.10	0.05
Very large	0.70	0.30	0.20	0.10

330

331 The EGA model has been originally developed with ArcGIS 10.1 (©ESRI) and updated
 332 with ArcGIS 10.8 (©ESRI). The toolbox is freely available for download on the website
 333 *www.woodflow.ch*.

334

335 **3.4 The Fuzzy-Logic GIS approach (FGA)**

336 The areas prone to landslides and debris flows were defined based on the linear trajectories
 337 provided by the SilvaProtect-CH database. To transform these lines into areas (i.e., pixels, as the
 338 FGA is entirely raster based), the density of the lines was used to classify the terrain into three
 339 intensity scenarios (section 3.5). High trajectory density was assumed to represent areas that are
 340 more prone to landslides or debris flows, more likely of a higher frequency and therefore, lower
 341 magnitude. Low trajectory density was assumed to represent areas that are less prone to mass
 342 movements, more likely affected by higher magnitude and thus lower frequency events. The
 343 thresholds to classify the three areas was based on four natural breaks (Figure S1A in
 344 supplementary material). In the case of mass movements, the delivery of wood to the stream
 345 network depends not only on the area of the landslide, but also on its connectivity to the channel
 346 (Ruiz-Villanueva et al., 2014c). Once the trajectories were converted to density pixels, the
 347 connectivity between these pixels and the stream network was established for landslide-prone
 348 pixels, as a function of both the distance to the channel and the terrain slope. In addition, a buffer
 349 area of influence was also established around these areas, to include toppled trees that may be
 350 recruited indirectly by the action of landslides. Trees located in a landslide-prone pixel or in the

351 toppling influence area (defined as a buffer equal two times the mean tree high; [here 100 m](#)), may
352 reach the channel if they were close enough (Euclidean distance [to channel network](#) < -50 m) or
353 further away ([Euclidean distance up to 100 m](#)) but on a steep slope (>40%). In the case of debris
354 flows, all pixels were assumed to be connected to the stream network.

355 Areas prone to bank erosion were computed based on channel sinuosity and gradient (as
356 proxies for channel lateral migration and transport capacity; Ruiz-Villanueva et al., 2014c), the
357 channel width and a defined width ratio. The width ratio was used to estimate the potential
358 resulting channel width after bank erosion during floods. It was calculated analysing an European
359 database (Ruiz-Villanueva et al., *in prep.*), including several rivers and flood events in
360 Switzerland and other 6 countries, and three scenarios were defined for different channel width
361 classes (9 classes ranging from < 3 to > 50 m). The stream network provided by the
362 ecomorphology database (section 3.2.1) was grouped by the channel width classes considered and
363 the width ratio was assigned to estimate the resulting potential erodible width for each stream
364 segment (Figure S1). The width ratio (ranging between 1 and 4) generally increases with scenario
365 intensity and decreasing channel width. The resulting buffers were transformed to pixels and the
366 final pixels prone to bank erosion were assigned based on channel sinuosity and gradient. Stream
367 segments characterized with high sinuosity and high gradient were assumed to be more prone to
368 bank erosion.

369 The described variables (i.e., landslide prone areas, connectivity, debris flow prone areas,
370 bank erosion prone areas, sinuosity and gradient) were transformed to fuzzy sets using the Fuzzy
371 Membership tool initially developed in ArcGIS 10.1 and updated to ArcGIS 10.7 (©ESRI) with
372 a linear membership function. The resulting converted fuzzy variables were combined (e.g.,
373 landslides prone pixels and connectivity; sinuosity and gradient) with the Fuzzy Overlay tool
374 (©ESRI). As a result, all pixels were transformed to fuzzy values ranging from 0 to 1; they were
375 then used to compute the volume of wood by multiplying the fuzzy pixel value by the forest
376 density pixel value (section 3.2.3). In case of overlapping pixels, priority was given to areas prone
377 to debris flows, then bank erosion and finally landslides (as in the EGA approach). The final

378 calculation considered also the accumulated wood load within the river network, but applying a
379 slightly different approach than for the EGA. This was estimated by assigning wood load values
380 based on [the](#) literature (Ruiz-Villanueva et al., 2016) to the different river segments grouped by
381 stream order classes [following the approach of Wohl \(2017\)](#) (i.e., < 3 stream order: $60 \text{ m}^3 \cdot \text{ha}^{-1}$;
382 between 3 and 6 order: $120 \text{ m}^3 \cdot \text{ha}^{-1}$; > 6 order: $50 \text{ m}^3 \cdot \text{ha}^{-1}$) and multiplied by fuzzy layers.

383 **3.5 Model scenarios definition**

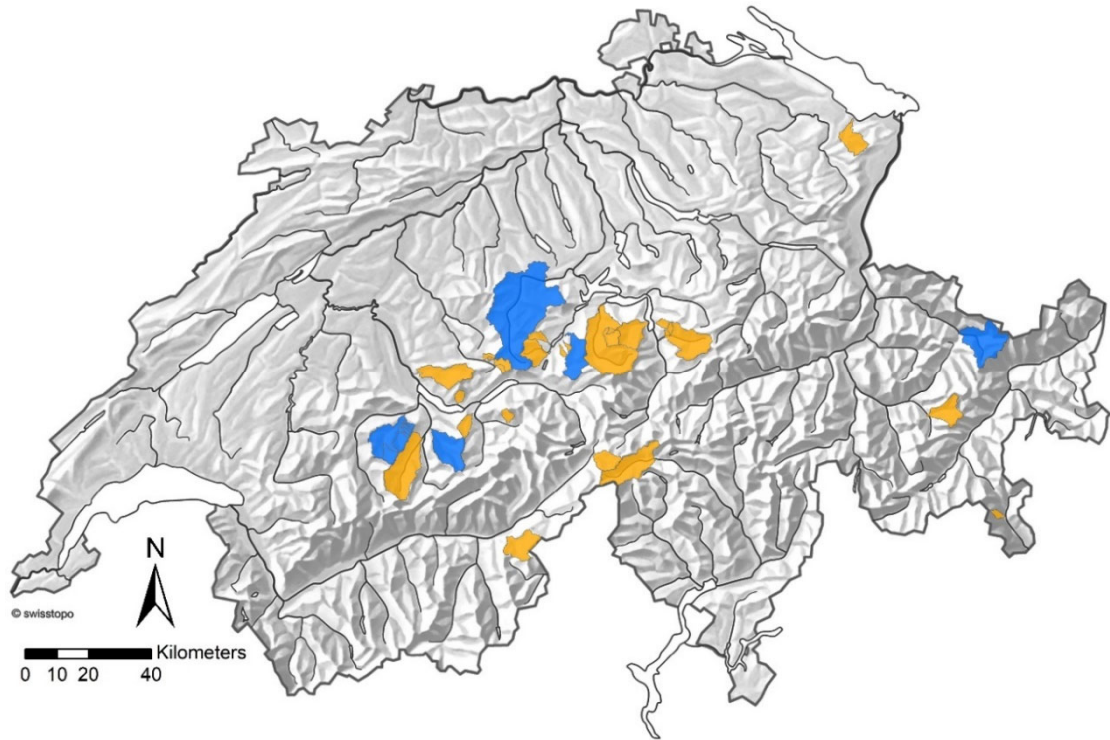
384 Three different scenarios were designed to estimate supplied wood volumes, based on a
385 qualitative assessment of the frequency and intensity of the wood recruitment processes involved.
386 These scenarios are called: medium scenario (medium-to-high frequency and intermediate
387 magnitude), large scenario (relatively low frequency and medium-to-high magnitude), and very
388 large scenario (very low frequency and very high magnitude).

389 Most of the documented floods with LW occurrence that were used to validate the GIS
390 models had a precipitation and/or peak runoff return period of 50-150 years, which was assigned
391 to the large volume scenario. The other two scenarios refer to approximate return periods and
392 were determined using *ad hoc* volume reduction factors (EGA) or the fuzzy logic rules (FGA),
393 because they could not be quantified more precisely due to a lack of data.

394 In addition to the estimated supplied wood volumes for each scenario, a potential wood
395 volume was also computed. The potential volume was assumed to be the maximum wood volume
396 supplied at the catchment scale, computed without any reduction by a coefficient (EGA) or by the
397 fuzzy logic values (FGA).

398 **3.6 Test catchments**

399 In the 40 catchments analysed in this work (Figure 3), considerable amounts of LW were
400 recruited and transported during past floods, and the resulting LW volumes were well documented
401 (mainly from the August 2005 flood; Rickli et al. 2018 and Steeb et al., 2017b). Table S1 in the
402 supplementary material provides an overview of the 40 test catchments and their characteristics.



403

404 **Figure 3: Location of the 40 test catchments (orange; with many nested sub-catchments). The**
 405 **five catchments in blue (Chiene, Chirel, Grosse Melchaa, Landquart, Kleine Emme) were used to**
 406 **calibrate the volume reduction factors from the EGA approach so that the estimated supplied wood**
 407 **was in the same order of magnitude as the observed values from past flood events.**

408

409 3.7. Model results analysis

410 Model results were first compared to observed wood volumes during floods, and then
 411 analysed in terms of (modelled) wood volumes per scenario, potential wood volume, wood
 412 volume supplied by different recruitment or supply processes (i.e., landslides, debris flows and
 413 bank erosion), and the estimated instream wood volume.

414 Statistical analyses were realized with the software RStudioVersion 2021.9.0.351 (R Studio
 415 Team, 2021). Differences between the two models and between them and the available
 416 observations were analysed in terms of mean values, standard deviation (SD) and root mean
 417 square error (RMSE), and tested by the nonparametric Wilcox (Mann-Whitney) or Kruskal-
 418 Wallis tests for two or more groups respectively (Stats package; R Core Team, 2019). Differences
 419 in the distributions of observed versus estimated wood supply volumes ('large' scenario) were as

420 tested using the Kolmogorov-Smirnov Test. Significance was set to a p value <0.05. The
421 dependence of wood volume on catchment controlling variables was verified by means of scatter
422 plots, regression analysis and correlation (*ggally* package; Schloerke et al., 2021).

423

424

4 RESULTS

425

4.1 Comparison between model outputs and model approaches

426

(EGA/FGA)

427

The two GIS approaches provide geospatial outputs – EGA in the form of feature class

428

polygons and the FGA in pixel-based raster files – that can be visualized on a map, as shown in

429

Figure 4. Potential recruitment areas for debris flow, landslide and bank erosion are generally

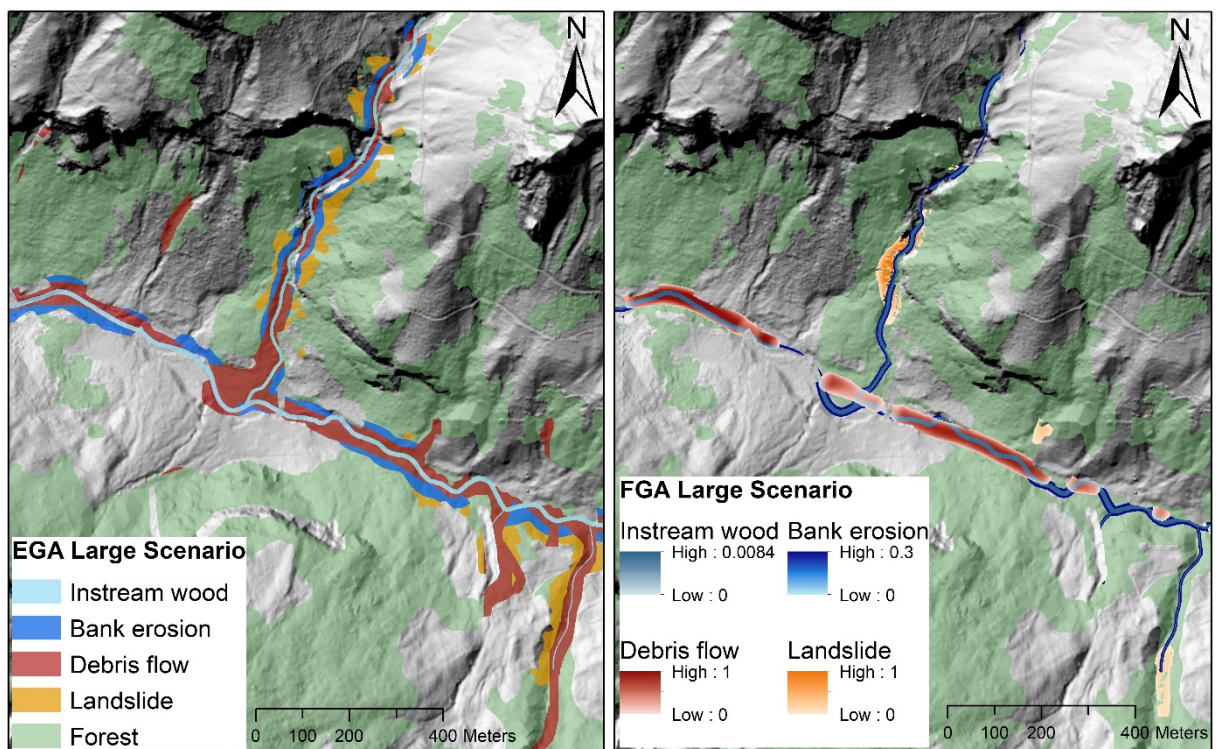
430

larger for EGA, i.e., the defined EGA buffer widths provide more supply-prone areas than the

431

respective combination of FGA fuzzy layers within the same perimeter.

432



433

Figure 4: Large volume scenario comparison of model outputs from EGA (left) and FGA (right)

434

at the Spiggebach torrent within the Chiene river catchment (Canton Bern). Potential recruitment

435

areas are shown for landslides (orange), debris flows (red), and bank erosion (dark blue). The stream

436

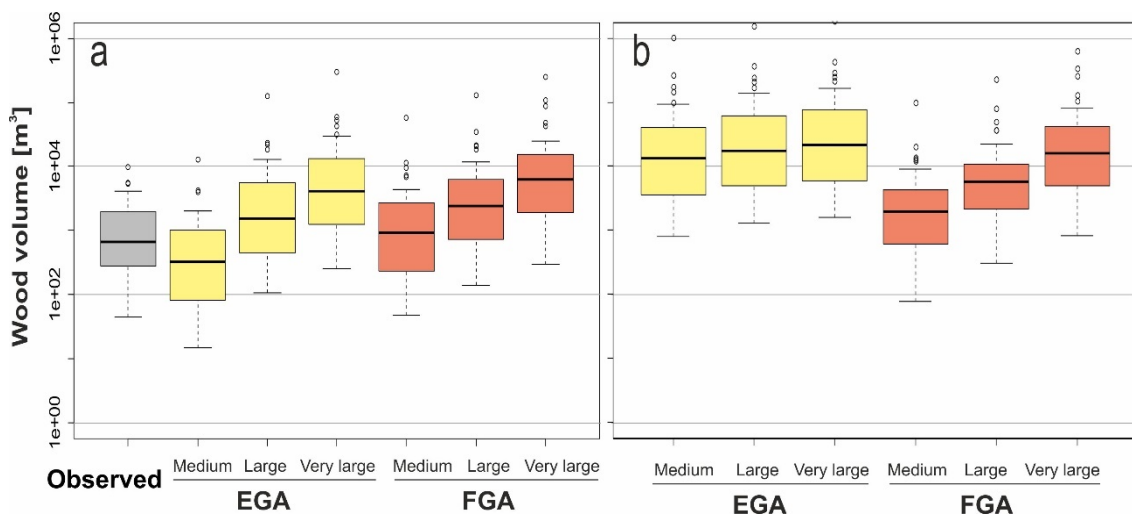
network (light blue) includes also instream wood loads. Background: Digital terrain model

437

(hillshade), © swisstopo.

438 The estimated supply and potential wood volumes for the three scenarios and the two models
 439 are shown in Figure 5 together with the available observations. The comparison between modelled
 440 and observed wood volumes is presented in section 4.3, the focus here is on differences between
 441 the two models. In general terms, Figure 5a highlights that the estimated supply wood volumes
 442 for each scenario were larger when computed by the FGA and lower by the EGA. For example,
 443 for the medium scenario, the averaged wood volumes were 994 m³ and 3318 m³ for EGA and
 444 FGA, respectively. The differences were slightly reduced for the other two scenarios, for which
 445 volumes equal to 7127 m³, 17353 m³, 8199 m³ and 19712 m³ were obtained (for the large and
 446 very large scenarios and the EGA and FGA, respectively; Table 3).

447 The variation in estimated wood supply is similarly high for both models, as shown by the
 448 statistical values in Table 3. Except for the maximum value of the ‘very large’ scenario, FGA has
 449 generally slightly larger percentile values. The standard deviation for the ‘large’ scenario of EGA
 450 is 20260 for EGA, and 20792 for FGA. The eEstimated wood supply volumes of EGA and FGA
 451 correlate well with only narrow scattering (Figure S6A), and the residuals similarly increase
 452 similarly with increasing catchment size (Figure S6B).



453 **Figure 5: Boxplots of wood supply (a) and potential (b) volume (m³) estimated by the two models**
 454 **EGA and FGA, and the three scenarios (i.e., medium, large, very large). “Observed” refers to the**
 455 **reported LW volumes after flood events (n=40; shown in grey color), in most cases equivalent to the**
 456 **large scenario.**

457 Observed LW supply during past events for all studied catchments (n=40) is given in grey color in
 458 panel (a).

460

Table 3: Statistical values of observed and estimated LW supply volumes for the three scenarios (i.e., medium, large, and very large) and the two models (i.e., EGA and FGA) for all studied catchments. “Observed” refers to the reported LW volumes after flood events, in most cases equivalent to the large scenario.

Wood supply volume [m ³]	Observed	EGA			FGA		
		Medium	Large	Very large	Medium	Large	Very large
Min.	45	15	106	253	48	141	300
1st	290	83	475	1378	244	764	2037
Median	673	329	1562	4189	921	2430	6342
Mean	1428	994	7127	17353	3318	8199	19712
3rd	1906	967	5161	12609	2588	6083	15191
Max.	9741	12757	126648	296893	57152	128575	249256
<u>Standard deviation (SD)</u>	<u>1927</u>	<u>-</u>	<u>20260</u>	<u>-</u>	<u>-</u>	<u>20792</u>	<u>-</u>
<u>Root Mean Squared Error (RMSE)</u>	<u>-</u>	<u>-</u>	<u>20225</u>	<u>-</u>	<u>-</u>	<u>21052</u>	<u>-</u>

Significantly higher values were computed for the large and very large scenarios compared to the medium scenarios, with a similar pattern shown by the two models. Larger differences were observed when comparing the estimated potential volumes (Figure 5b and Table 4). In this case the EGA resulted in much higher values than the FGA (especially for medium and large scenarios), which is a result of much larger potential recruitment areas (Figure 4) Accordingly, the percentile values of EGA potential LW supply volumes shows more variability. Figure S3 shows that for EGA, the estimated LW supply volume corresponds to 8 % of the potential wood supply volume on average. In the case of FGA, this ratio varies much more with an average of 47 %.

Table 4: Potential LW supply volumes for the three scenarios (i.e., medium, large, and very large) and the two models (i.e., EGA and FGA) for all studied catchments.

Potential wood volume [m ³]	EGA			FGA		
	Medium	Large	Very large	Medium	Large	Very large
Min.	807	1289	1601	76	305	811
1st	3529	4949	6000	613	2203	5341
Median	13226	17579	21619	1965	5774	15965
Mean	58664	86984	105723	5961	16173	52995
3rd	37672	59612	74948	4207	10665	41066
Max.	1011306	1534850	1866295	100165	231336	632151

4.2 Contribution from different supply processes

The main difference between the two models was the estimated contribution from each supply process to the obtained wood volume. Landslides were the dominant process in the case of the EGA, with a contribution up to more than 60% of the computed wood volume (for the large scenario); whereas bank erosion was the predominant process in the FGA model for all scenarios (Figure 6). Debris flows played an intermediate role in supplying wood according to the two models; however, the importance of this process varied depending on the scenario. For the medium scenario, the EGA model showed a similar percentage of averaged wood supplied by landslides and debris flows. The FGA, contrastingly, computed most of the averaged wood volume supplied by bank erosion, and only a low percentage of wood supplied by landslides and debris flows. Only for the very large scenario, the importance of landslides, in terms of percentage of supplied wood, equaled or even exceeded, the volume estimated from bank erosion with the FGA.

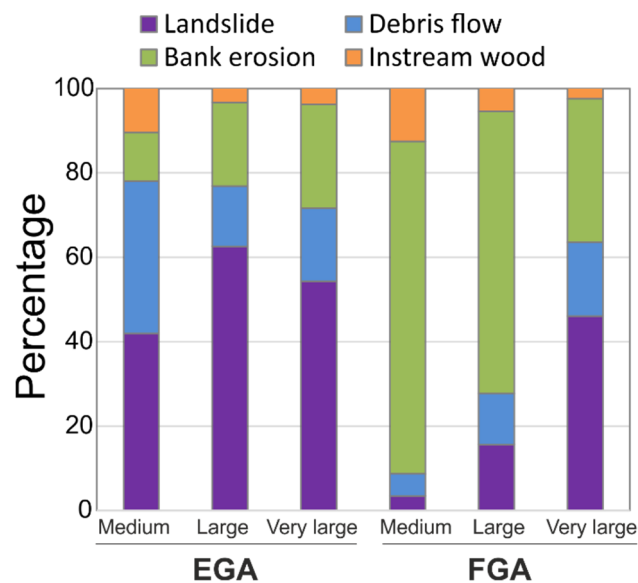
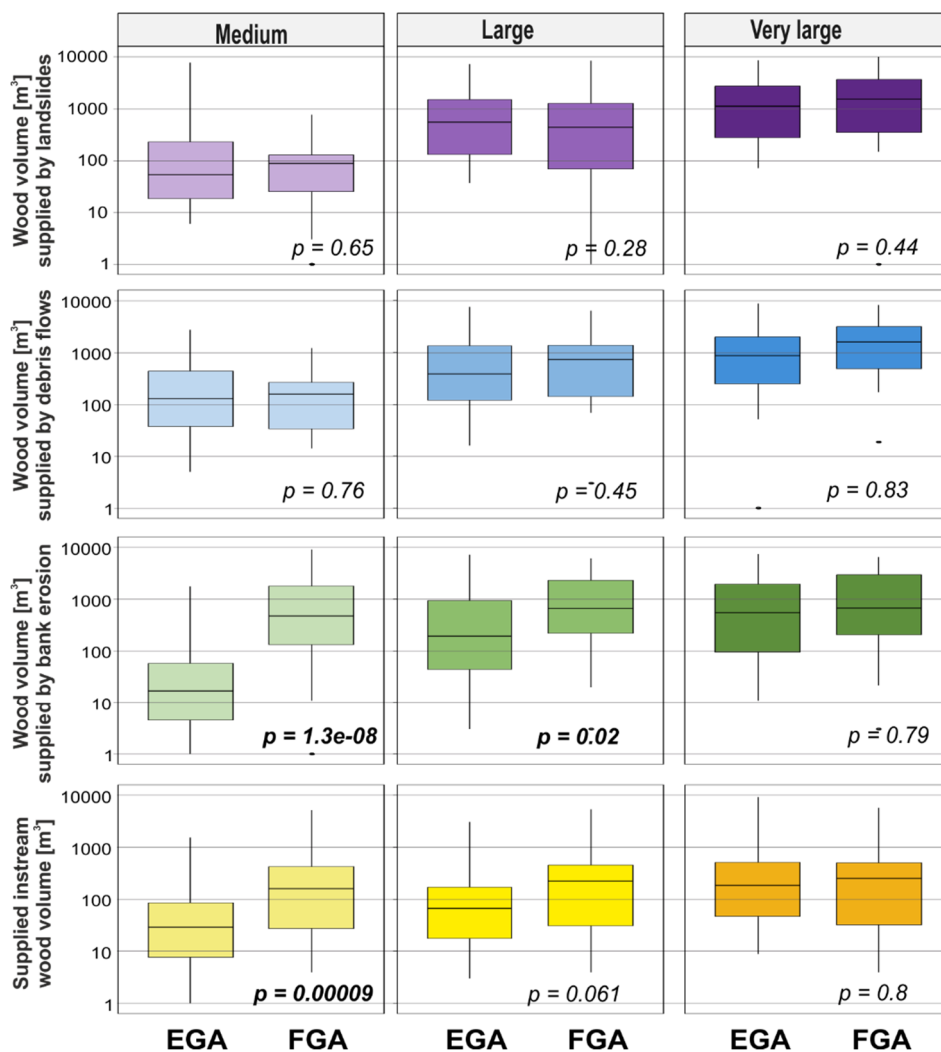


Figure 6: Large wood volumes supplied by each process, model, and scenario averaged for all 40 study sites.

The difference between the contribution of each process to the estimated volumes is clearly shown in Figure 7 and 8 (with FGA resulting in generally higher volumes than EGA). The graph illustrates that statistically significant differences were found between the computed supply wood

499 volumes by the two models and by bank erosion process. The median wood supply values (see
 500 black lines within boxplots of Figure 7) are about a factor of 1000 and 10 larger for the FGA than
 501 for the EGA, and for the medium and large scenarios respectively. This explains the relative
 502 dominance of bank erosion for the FGA (see also Figure 8), for the medium and large scenario.
 503 The wood volumes supplied by the other processes were not significantly different between the
 504 two models. Only the estimated instream wood volume for the medium scenario showed a
 505 significant difference between the EGA and the FGA, with larger volumes computed by the latter.
 506

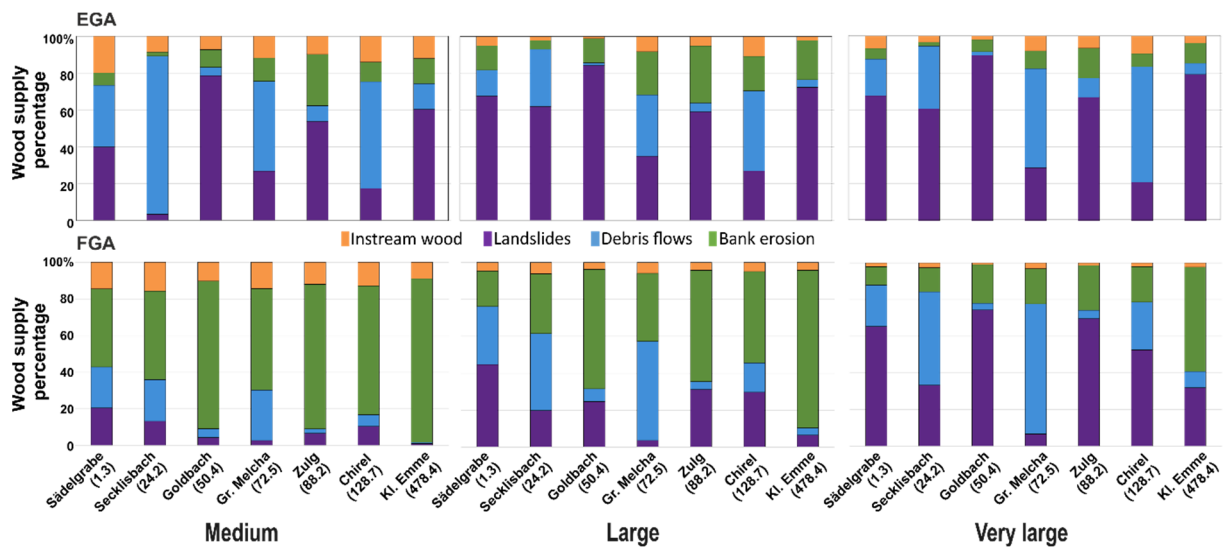


507

508 **Figure 7: Wood volumes supply estimated for landslides, debris flows, bank erosion, and**
 509 **estimated supplied instream wood by the two models and the three scenarios. The p-value is from the**
 510 **Wilcoxon test (significant values shown in bold).**

511 However, the contribution of each process to the computed wood volume did not only vary
 512 according to the model, but also according to the site. Figure 8 shows a selected sub-dataset of
 513 catchments with different drainage areas, revealing the large variability of the dominant wood
 514 supply process, and the dominance of different processes over the others in the two models. In
 515 general, the FGA approach shows a larger contribution from landslides and debris flows in smaller
 516 catchments, while landslides are the major contributor to wood supply regardless the catchment
 517 size for the EGA. Bank erosion is a minor contributor to the estimated supply in EGA for most
 518 sites and irrespective of the scenario used. However, bank erosion is the most relevant process for
 519 the FGA, which is clearly illustrated by the Kleine Emme River catchment, the largest of the study
 520 sites of the dataset, for which the FGA estimates the largest contribution by this process. The
 521 EGA model, on the other hand, estimated a larger contribution from landslides for this site.

522 The proportion of instream wood loads remains constant, independent of catchment size (2-
 523 13 % of total wood supply). The contribution of debris flows and landslides are highly variable
 524 depending on topography, and can be dominant for small (e.g., Secklisbach) or large catchments
 525 (e.g., Grosse Melchaa or Chirel).



526

527 **Figure 8: Percentage of wood volume supplied by each process, model, and scenario for selected**
 528 **studied sites, the names and catchment area in (km²) are provided in the abscissa.**

529

4.3 Estimated and observed wood volumes

The comparison between observed LW volumes V_{obs} and estimated (modelled) LW volumes V_{est} are shown in Figure 9a. There is a relatively large scattering when comparing observed and estimated wood loads. Both under- and overestimation of V_{obs} are observed for both models, with a larger tendency for overestimation. Overestimation remains generally within two orders of magnitude (typically higher values for FGA), underestimation within one order of magnitude (typically lower values for EGA).

Figure 9b further shows the ratio of V_{est}/V_{obs} versus catchment area. Both under- and overestimation of V_{obs} are present over >2 order of magnitude for all catchment areas. However, in general, overestimation increases with increasing catchment size for both models. There is a shift around a catchment area of 7 km², above which overestimation is significantly larger (with a factor of >10). In catchments with areas less than 7 km², estimated wood supply is generally underestimated (see dashed line in Figure 9b).

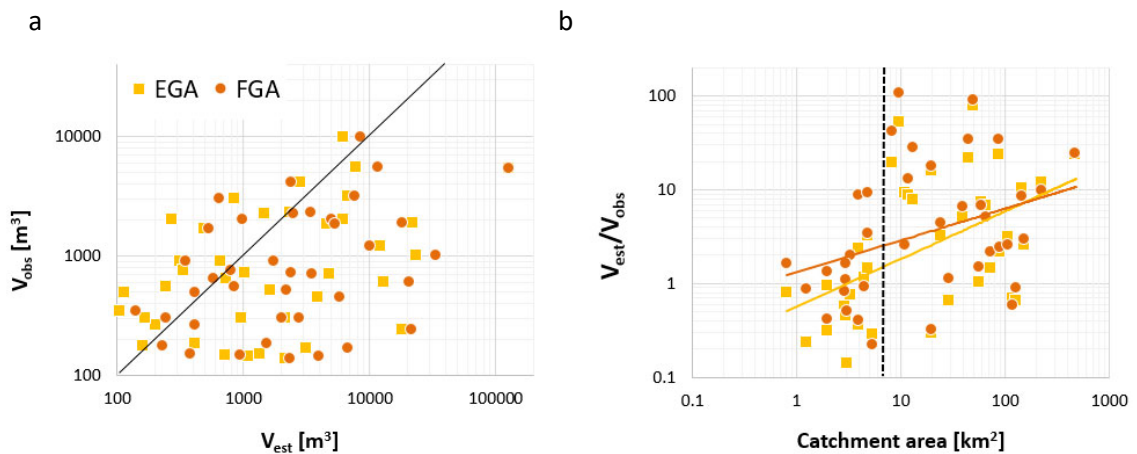
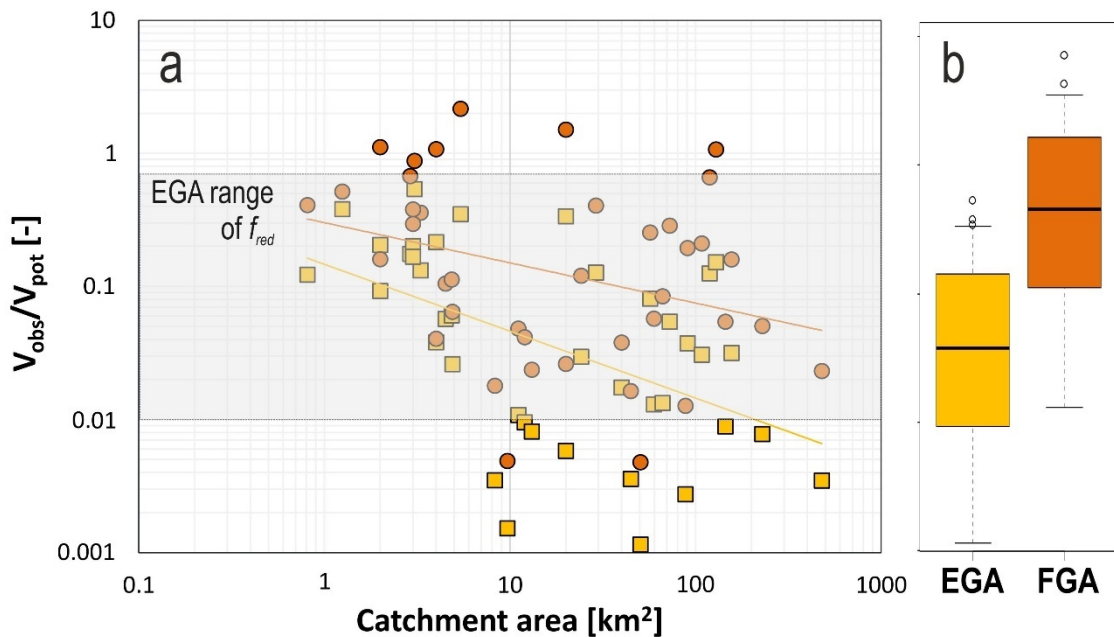


Figure 9: Left: Modelled LW V_{est} (large scenario) versus observed wood volume V_{obs} during past events. The black line shows the line of equality (1:1 line). Right: Ratio of V_{est}/V_{obs} versus catchment area.

This tendency of overestimation with increasing catchment size can also be explained by comparing the ratio of observed and potential wood volume V_{obs}/V_{pot} versus catchment area (Figure 10a). With increasing catchment size, there is a trend of decreasing ratio values of V_{obs}/V_{pot} . This means in larger catchments, the volume reduction factors (FGA) and the fuzzy rules

553 (FGA) are often not small enough to reduce the wood potential accordingly, creating
554 overestimation of wood volumes ($V_{est} > V_{obs}$).

555 Since potential wood volumes are much higher for EGA (Table 4 & Figure 5b), the ratio of
556 V_{obs}/V_{pot} is also much smaller in case of EGA (almost one order of magnitude difference as shown
557 in Figure 10b). For FGA few examples (i.e., six orange dots in Figure 10a) exist for which the
558 potential wood volume is even smaller than the observed wood volume ($V_{obs}/V_{pot} > 1$).



559

560 **Figure 10: Ratio of observed wood volumes and potential wood volumes computed by the two**
561 **models for all sites and their catchment areas. The grey rectangle shows the reduction factor range**
562 **used for EGA computations.**

563

564 ~~Differences in distributions of observed versus estimated wood supply volumes ('large'~~
565 ~~scenario) was tested using Kolmogorov-Smirnov Test (Table S3). A statistically different~~
566 ~~distribution could only be observed for the FGA compared to the observed values. Only for FGA~~
567 ~~versus observed values, a statistically different distribution could be identified. The comparison~~
568 ~~between the values obtained by the EGA vs and those observed values one, and between the~~
569 ~~values obtained by EGA vs and those obtained by FGA obtained values, showed no significantly~~
570 ~~different distributions (Table S3). This outcome is also visualized/illustrated in the histograms of~~
571 ~~Figure S7.~~

573 5 DISCUSSION

574 5.1 Major differences between the two models and remaining challenges

575 Both the EGA and FGA are based on a similar general concept, were fed with similar input
576 data (e.g., stream network, forest density, areas affected by landslides and debris flows) and run
577 with defined equivalent scenarios which made the comparison possible. However, there are also
578 some methodological differences that resulted in different model outputs. Here we describe them,
579 while in the following section we discuss our results comparing them to current knowledge and
580 other existing methodologies.

581 The most relevant difference between the EGA and FGA is the approach to define the areas
582 affected by **bank erosion**, thus the contribution of this recruitment process and the estimated
583 wood supply volumes. EGA uses buffers around the stream network computed for each scenario
584 with one specific width factor, independent of the original channel width. The resulting buffer
585 widths were added on both sides of the original channel width (section 3.3). FGA also assigned
586 scenario-specific buffers, computed with width ratios that vary according to nine channel width
587 classes (Figure S1). Half of the resulting buffer widths were added on both side of the original
588 channel width. As a result, potential bank erosion recruitment areas are generally larger for EGA
589 than for FGA. However, the reduction factors used for the EGA assumed that between 5% and
590 20% of the potential wood volume within these areas contribute to the estimated wood supply,
591 which resulted in a much lower estimated wood volume. In the case of the FGA, the entire forested
592 area identified as prone to bank erosion along the river network is contributing to wood supply
593 and the volume is reduced based on fuzzy logic pixel values (computed based on sinuosity and
594 channel slope, and going up to 30% of the potential), which resulted in a much larger volume.
595 This difference is particularly relevant for the medium scenario, for which the bank erosion width
596 identified by both models are quite similar, but the resulted wood volumes significantly differ
597 (e.g., average wood volume equal to 114 and 2613 m³ for EGA and FGA respectively for all
598 sites). Moreover, the erodibility of the channel banks was not considered in the models. Anthropic
599 elements such as like bank protections, check-dams, and bridges or the presence of bedrock may

600 limit bank erosion and widening, and thus wood supply. This information was not available at the
601 required resolution and spatial scale for the catchments analysed~~river catchments, and thus we~~
602 could therefore not be included~~it~~. This also results in an overestimation of the computed wood
603 volumes due to~~by~~ bank erosion, which ~~may~~could be more relevant in the FGA than in the EGA
604 (for which the volume reduction coefficient could be more easily adjusted)~~This difference in the~~
605 ~~way of computing recruitment areas from bank erosion and related wood volumes explains the~~
606 ~~second most important difference between the two models.~~

607 As shown in section 4.2, landslides are the **dominant recruitment process** in the case of the
608 EGA, whereas bank erosion is the predominant process in the FGA model. In both models, for
609 landslides and debris flows, the input data were the trajectories from the SilvaProtect-CH
610 database, but the EGA applies an expert-based buffer for each scenario to those trajectories, while
611 the FGA groups them in three classes according to their density. In addition, the fuzzy
612 connectivity applied in the FGA further reduces the areas identified as prone to mass movements
613 (only for landslides). This hillslope-channel network connectivity is another methodological
614 difference between the two models. In EGA, as a proxy for connectivity, only landslide
615 trajectories within 50 m distance from the stream network were considered. FGA considers
616 connectivity as a function of both the distance to the channel and the terrain slope (as used by
617 Ruiz-Villanueva et al., 2014c). Noteworthy, both models use Euclidean distance, but no
618 geomorphometric measures (e.g., steepest downslope direction) as often used to assess sediment
619 connectivity (e.g., Cavalli et al., 2013).

620 The EGA generally produces much larger potential recruitment areas for landslides and
621 computes larger wood supplied by landslides than the FGA, for all three scenarios. For the FGA,
622 landslides are minor supplier of wood for the medium and large scenarios, while their contribution
623 for the very large volume scenarios significantly increases.

624 Existing observations show that mass wasting processes, such as debris flows and landslides,
625 often are the most relevant recruitment processes in smaller headwater catchments (e.g., Rigon et
626 al., 2012; Hassan et al., 2016; Seo et al., 2010). In contrast, (lateral) bank erosion is often prevalent

627 farther downstream in larger mountain or lowland rivers, resulting in large volumes of LW supply
628 by this fluvial recruitment process. This was observed after the large flood in 2005 in Switzerland
629 (Steeb et al., 2017b), the large flood in the Magra River catchment in Italy in 2011 (Lucía et al.,
630 2015c; Comiti et al., 2016) and along the Emme river catchment in 2014 (Ruiz-Villanueva et al.,
631 2018). In smaller streams, bank erosion and channel widening can also be significant, especially
632 in natural reaches (no stream regulation works), as seen after severe flash floods in Braunsbach,
633 Germany in 2016 (Lucía et al., 2018). In most of these cases, only a small proportion (<30%) of
634 the total recruited wood was supplied by mass wasting processes, and the majority of the supply
635 was due to bank erosion and channel widening along the river network.

636 Such catchment size-specific trends of dominant recruitment processes are not clearly
637 prevalent in the model results of EGA and FGA. Generally, the variability in the recruitment
638 processes and thus in the wood supply is very large, both in empirical data as well as in modelling
639 results, highlighting the importance of other catchment- and event-specific characteristics. The
640 relationship of estimated LW supply with catchment characteristics is shown in supplementary
641 material Figure S2. The highest correlation is seen for forested stream length that can be
642 interpreted as a proxy for potential supply volume for bank erosion. High correlations also exist
643 for Melton ratio and relief ratio, both surrogates for watershed slope, a factor that is directly
644 related to stream power and debris flow and landslide propensity. In general, V_{obs} from EGA
645 shows slightly higher correlations (R^2) with catchments characteristics than FGA. More research
646 is needed to better understand wood recruitment processes and to improve predictive models on
647 a physical basis. This will help to determine where and how likely mass wasting (landslides) or
648 bank erosion could occur.

649 The results in section 4.3 indicate that there is both under- and overestimation of wood supply
650 volumes. As shown in Figure S4, potential LW supply V_{pot} generally increases with catchment
651 size. During a convective storm event, often only a part of the catchment is affected, and therefore
652 geomorphologically active, so that LW supply may easily be overestimated ($V_{est} > V_{obs}$). In
653 smaller catchments and torrents, sporadic recruitment processes such as landslides or debris flows

654 can dominate and deliver large amounts of wood at once, so that wood supply may be
655 underestimated by our models ($V_{est} < V_{obs}$).

656 Another important aspect regarding the overestimation of the calculated/computed wood
657 volumes by the FGA and EGA is the assumption that the estimated volumes are supplied and
658 exported to the outlet of the catchment, which may not be the case if the wood is being deposited
659 along their way. The models do not consider the transfer of the wood along the river network
660 (as, for example, in the approaches of Franceschi et al., 2019 or Zischg et al., 2018).

661 A less relevant difference between the models, and in terms of the total contribution to the
662 wood volume estimations, is the approach used to assign previously **deposited instream wood**
663 **loads**. The EGA assigns instream wood load values into three channel width classes (section
664 3.3), whereas FGA assigns wood load values into three stream order classes (section 3.4). The
665 main divergence comes from the assumption that the smaller channels contain the largest instream
666 wood load for the EGA (following observations in 10 small mountain streams in Switzerland
667 from Rickli et al., 2018), while the FGA assumes that larger loads are present in medium order
668 channels (as proposed by Wohl, 2017). Despite the different approaches, both models used
669 empirical data from Ruiz-Villanueva et al. (2016) to assign volumes, and the resulting wood load
670 volumes were only significantly different in the case of the medium scenario (Figure 7).

671 These differences in the methodologies result in differences in the outcomes, in terms of the
672 **potential and estimated wood supply**. The EGA generally produced larger potential recruitment
673 areas. The volume reduction factors applied in EGA are, however, on average much smaller than
674 the respective fuzzy-logic values created in FGA (Figure S3). As a result, estimated wood supply
675 is generally larger for FGA, as shown in section 4.1. For our test catchments, the application of
676 simple empirical volume reduction factors as part of the EGA model has proven to be similarly
677 accurate in estimating LW volumes, in comparison with a spatially explicit approach such as the
678 FGA model. Still, both the expert-based buffer widths and the reduction factors were defined for
679 the test catchments and validated for similar catchments located in the Alps and pre-Alps, and so
680 they should be carefully tested if applied to other rivers with different characteristics. The fuzzy

681 logic approach indirectly includes this uncertainty or imprecise information (i.e., buffer widths
682 and volume reduction factors), and allows being computed without prior existing observations or
683 knowledge. In both cases, the two models may over- or underestimate the wood volumes, but
684 allow reliable computation of wood supply volumes at the catchment scale and for three scenarios.

685

686 **5.2 Qualitative comparison of EGA and FGA with other similar** 687 **approaches**

688 As described in the introduction, ~~just only~~ a few approaches have been proposed to compute
689 wood supply at the catchment scale considering different recruitment processes (e.g., landslides,
690 debris flows, bank erosion). ~~As those models presented here, most~~ Most of the model frameworks
691 described in section 2, particularly those based on GIS and geoprocessing (e.g., Mazzorana et al.,
692 2009), do not attempt to simulate the actual recruitment processes, but ~~they used~~ existing
693 information on areas susceptible to certain processes (~~likeas~~ the EGA and FGA) from hazard
694 maps or other sources or apply expert-based buffers (~~likeas~~ the EGA). Most existing models
695 simulate only one recruitment process explicitly, i.e., landslides or bank erosion (Lucía et al.,
696 2015a; Cislaghi et al., 2018; Zischg et al., 2018; Gasser et al.; 2018, 2020), and a few consider
697 mass movements and fluvial processes (e.g., Franceschi et al., 2019). ~~Very few models simulate~~
698 ~~only one recruitment process (i.e., landslides or bank erosion) explicitly (Lucía et al., 2015a;~~
699 ~~Cislaghi et al., 2018; Zischg et al., 2018; Franceschi et al., 2019; Gasser et al.; 2018, 2020).~~ Yet,
700 a model that simulates coupled processes to compute wood supply is still lacking. In existing
701 approaches, physically based models are combined with empirical approaches to identify
702 recruitment areas from one single process and compute wood supply at the catchment scale. Still,
703 these models require additional input data, such as precipitation, discharge, soil characteristics
704 etc., which is usually not available or challenging to be obtained at the desired resolution. In addition,
705 they are much more expensive in terms of computational time, which limits their application to
706 larger areas. Therefore, there is a gap between the current state-of-the-art of geomorphic process
707 modelling and wood recruitment and supply estimation.

708 Moreover, the majority of existing models used to predict wood supply are deterministic,
709 in that they do not consider the natural process variability and parameter uncertainties. Only the
710 fuzzy logic approach (Ruiz-Villanueva et al., 2014c; Ruiz-Villanueva and Stoffel, 2018)
711 indirectly considers uncertainty, but it does not represent a description of the physical supply
712 processes. A few stochastic models have been proposed (e.g., Bragg, 2000; Eaton et al., 2012;
713 Gregory et al., 2003) to simulate wood recruitment, but they were designed to work at the scale
714 of the river reach only. At the catchment scale, a probabilistic multi-dimensional approach has
715 recently been proposed (Cislaghi et al., 2018) to study wood sources from hillslopes, modelling
716 areas susceptible to landslides, but it neglects other processes such as bank erosion. The latter
717 process has been considered in one of the most recent studies on LW (Gasser et al., 2020).

718 On the other hand, empirical estimation formulas (e.g., Steeb, 2018; Rickenmann, 1997;
719 Uchiogi et al., 1996) are easier and faster to apply to estimate LW supply. However, they provide
720 only an estimate for the whole catchment under investigation, without any spatial differentiation.
721 EGA and FGA, on the other hand, support a comprehensive spatial overview and direct attention
722 to areas in which a more precise assessment of the instream wood situation is necessary, e.g.,
723 through field surveys or expert assessments. Figure S5 shows that the EGA and FGA modelling
724 results approximately correspond to the 50-90% relation between V_{obs} and catchment area as
725 described with the empirical formula of Steeb (2018).

726

727 **5.3 Uncertainty in the observed and modelled LW volumes**

728 The two GIS approaches presented here yielded similar orders of magnitude of LW supply
729 for a given catchment and for the three designed scenarios. Still, several uncertainties associated
730 with the estimation of LW supply remain, and they are not just related to the obtained results and
731 the applied methodologies, but also to the available observations (coming from surveys after flood
732 events) used for calibration and validation.

733 The observed wood volumes V_{obs} were compiled mostly from technical reports of post-
734 event analyses, and these values might be in some cases only rough estimates, with a considerable
735 uncertainty. LW volumes were estimated based on LW deposits and piles in the field, for which
736 the volume and the corresponding wood content (or pore volume, respectively) must be estimated.
737 The assessment of the wood volume of such accumulations might be challenging and uncertainty
738 might be high (Spreitzer et al., 2020; Thevenet et al., 1998). Some of the observed wood volumes
739 V_{obs} were also determined on the basis of forest loss areas, for which a pre-event forest density
740 value W must be assumed. In the analysis made with the GIS models, the forest density raster
741 map of Ginzler et al. (2019) was used, which may differ from values used during the post event
742 surveys. Furthermore, the time gap between a LW transporting flood event and the survey year
743 on which the forest density map is derived from, needs to be accounted for. Depending on this
744 relationship, wood volumes may be underestimated (i.e., survey year after flood event) or
745 overestimated (i.e., survey year before flood event). This circumstance could also explain why in
746 some cases of the FGA calculations the potential wood volume is even smaller than the observed
747 wood volume ($V_{obs}/V_{pot} > 1$; see Figure 10a). This discrepancy appeared mostly in one large
748 catchment (i.e., Chirel) and its subcatchments (i.e., Fildrich, Goldbach, Rütigrabe), and could be
749 related to the forest density data used to compute the wood supply volumes, which was computed
750 with the forest after the large flood in 2005.

751 The observations we used remain a unique and extensive dataset (Steeb et al., 2019a),
752 which allowed us to parametrize the models more accurately. The EGA uses empirical volume
753 reduction factors that were derived from this dataset for the conversion of V_{pot} to V_{est} . In case of
754 debris flows, for example, the volume reduction factors f also rely on an event analysis of the
755 August 2005 flood in Switzerland by Rickenmann et al. (2008), who showed that, on average, 11-
756 19 % of all torrents in the main investigated mountain river catchments were associated with
757 debris flow activity. This percentage range was used to define the reduction factors as shown in
758 Table 2. This highlights the importance of in-depth post flood event analyses, as these provide
759 valuable empirical datasets that can be used to validate and further develop models to estimate

760 supplied LW volumes. The application of models should not replace field work surveys, but they
761 should be used in a complementary manner.

762 Another source of uncertainty is given by the SilvaProtect-CH trajectories. Since their input
763 data, in particular geology, provide a large-scale representation of natural conditions (see text in
764 the supplementary material), the SilvaProtect-CH trajectories are best suitable for use on a
765 catchment-scale range. Furthermore, SilvaProtect-CH trajectories generally result in a pessimistic
766 picture under unfavourable conditions (e.g., no consideration of the stabilizing influence of
767 vegetation cover). As a consequence, only a small part of the trajectories is expected to be active
768 during rainfall and consequent floods. In addition, the actual run-out zones of mass wasting
769 processes may often be shorter than the modelled trajectories.

770 One important limitation of the EGA and FGA models presented in this study is that the
771 available input forest cover, does not provide any further information about the forest typology,
772 structure and species composition. Despite the role that differences in forest may play in
773 stabilizing the soil and slopes and in influencing bank erosion and hillslope stability (Gasser et
774 al., 2019), the two methods do not explicitly consider this effect. Moreover, the type, structure
775 and stage of forest stand control the extent to which trees can be uprooted and recruited and
776 supplied to rivers (Mazzorana et al., 2009; Ruiz-Villanueva et al., 2014c). This aspect was
777 described as the vegetation resistance defined by Ruiz-Villanueva et al. (2014c) based on the tree
778 species and forest stage, the structural classification of forested areas made by Blaschke et al.
779 (2004) and the availability indicator used by Mazzorana et al. (2009). Unlike in the approach used
780 by Franceschi et al. (2019) or Gasser et al.; (2018), who detected individual trees from high-
781 resolution LiDAR data, in our case,~~However,~~ there was no ~~available~~ information available with
782 the ~~required~~ spatial resolution required to take account for ~~consider~~ the dimensions, proportion of
783 different species, the stage (e.g., remnant or reforested) or the age of the forest stand. Neglecting
784 the different response of different forest types may result in an overestimation of supplied
785 volumes.

786 As discussed above, modelling and quantification of wood supply volumes is characterised
787 by many uncertainties. After all, the two models presented in this study allow quantifying the
788 magnitude of the expected LW supply, thus further expert judgement and knowledge of local
789 (geomorphic) characteristics is required to adequately interpret the results. The ratio between
790 predicted and observed LW volumes varies by about 1-2 order of magnitudes. For comparison it
791 is noted that a similar or even larger range of uncertainty can be expected for the estimation of
792 bedload volumes transported during floods (e.g., Rickenmann and Koschni, 2010).

793

794 **5.4 Implications for hazard assessment and river management**

795 From a practical perspective, geospatial LW modelling results can be used for hazard
796 assessment, infrastructure design, and the definition of management strategies. From a scientific
797 perspective, further applications are possible. For example, estimated wood volumes can be
798 applied as an input for a wood transport model, such as Iber-Wood (Ruiz-Villanueva et al., 2014a,
799 2014b, 2015) or other approaches (e.g., Mazzorana et al., 2011), to define realistic boundary
800 conditions. Furthermore, if no observation data are available for reference, estimated wood
801 volumes from EGA and FGA can be used to quantify blocking probabilities due to LW at bridge
802 piers or at other critical cross-section (Schalko, 2019; Schalko et al., 2018; Schmocker and
803 Weitbrecht, 2013).

804 As described in section 4.2, the average proportion of instream deadwood (instream wood
805 load) from the total potential LW supply in the 40 test catchments ranged between 2-13 % (Figure
806 6). This range is confirmed by other studies and event analyses (Dixon, 2013; Rickli et al., 2018;
807 Waldner et al., 2009). It can be concluded that instream deadwood generally accounted for only
808 a small proportion of the total LW transported during past floods in Switzerland. Rather, it is
809 freshly recruited wood that made up the majority of the transported wood volumes. Deadwood
810 alone, both on the forest floor and in the channel itself, may therefore only lead to a limited
811 increase in risk from a natural hazard management perspective. As a consequence, the artificial

812 removal of deadwood from the stream and its surroundings is not always necessary, keeping in
813 mind the ecological benefits of instream wood.

814 EGA and FGA are area-wide products that can be applied in any Swiss catchment. They
815 use a standardized procedure and nationwide homogeneous data, which facilitates a comparison
816 between catchments (FOEN, 2019). The methodology is flexible and can be adapted to other
817 regions outside Switzerland if recruitment processes (especially with regard to SilvaProtect-CH
818 trajectories) were modelled with more generic approaches.

819 Both models have been used already been used by practitioners for some engineering
820 applications. One limitation that has been identified encountered by some practitioners is the use
821 of licensed software, as both EGA and FGA have been were developed in ESRI software and
822 require need some advanced licenses that may ight not be always be available accessible to private
823 companies. Future developments may consider the migration to open-source software.

824 Furthermore, there is still a need to analyse and model the propagation of LW through the
825 river network, by for example by, applying hydraulic modelling (e.g., Ruiz-Villanueva et al.,
826 2014) or the recently proposed network approaches such as those applied to sediment transfer
827 (Finch and Ruiz-Villanueva, 2022).

828 The two models presented here correspond to a hazard index mapping in terms of
829 processing depth and degree of detail for a hazard assessment. The geospatial modelling results
830 indicate areas of potential LW recruitment, however without precise information about on the
831 intensities occurring or the transfer and propagation through the river network. In contrast, the
832 estimated LW supply for the large scenario is based on the data of events with a return period of
833 approximately 50 to 150 years. The approach presented here is a useful tool to give a
834 comprehensive overview and direct attention to areas where a more precise assessment of the LW
835 situation is probably useful, for example in connection with an estimation of sediment loads in
836 torrents.

837

838 6 CONCLUSIONS

839 Two GIS-based models are presented in this contribution to identify large wood (LW)
840 sources and to estimate LW supply to rivers. Both models, called empirical GIS approach (EGA)
841 and Fuzzy-Logic GIS approach (FGA), consider landslides, debris flows, bank erosion, and
842 mobilization of instream wood as recruitment processes. The results are volumetric estimates of
843 LW supply based on three different scenarios of process frequency and magnitude. Results of
844 model applications to 40 Swiss catchments were used to compare both the two models with each
845 other and the performance in relation to observed (empirical) LW volumes. Further, a literature
846 review of existing LW supply models proposed in the last 35 years was conducted, set into context
847 and remaining challenges were identified.

848 EGA shows significantly higher values for potential LW supply. However, after reducing
849 the potential volume with different methods, estimated LW supply volumes are in the same order
850 of magnitude for both models, with FGA showing generally somewhat larger values. In case of
851 EGA, landslides are the dominant recruitment process, whereas bank erosion is dominant for
852 FGA. Both models show under- and overestimation of observed wood volumes V_{obs} , with more
853 tendency for overestimation. Overestimation stays generally within two orders of magnitude
854 (typically larger values for FGA), underestimation within one order of magnitude (typically
855 smaller values for EGA).

856 The modelling and quantification of wood supply volumes is characterised by many
857 uncertainties. After all, the two models presented in this study allow quantifying the magnitude
858 of the expected LW supply, thus further expert judgement and knowledge of local (geomorphic)
859 characteristics is required to adequately interpret such results. LW supply modelling can be
860 further improved by integrating more physically-based and/or probabilistic inputs for the spatial
861 identification of recruitment processes. Likewise, the parametrization and validation of LW
862 supply models remain complex. Post flood event analysis provide valuable empirical datasets that
863 can be used to validate results and further develop LW supply models that can be useful for hazard
864 assessment, infrastructure design, and the definition of management strategies.

865 **ACKNOWLEDGEMENTS**

866 We thank the Swiss Federal Office for the Environment (FOEN) for funding the research
867 program "Large Wood Management in Rivers" (WoodFlow research program; contract no.
868 15.0018.PJ/O192-3154).

869 Special thanks go to Peter Waldner (WSL) for providing valuable empirical data from flood
870 events; Benjamin Kuratli (formerly University of Zurich) for helping to develop earlier versions
871 of the EGA; Bronwyn Price, Christian Ginzler and Markus Huber (all WSL) for providing data
872 from the Swiss National Forest Inventory; and finally, Stéphane Losey (FOEN) for providing all
873 the required SilvaProtect-CH data.

874

875 **REFERENCES**

- 876 Bachmann Walker, A. 2012. Ausmass und Auftreten von Seitenerosionen bei Hochwasser.
877 Auswertung von hydraulisch verursachten Seitenerosionen und Herleitung von empirischen
878 Zusammenhängen zur Ermittlung des Erosionsausmasses und -auftreten. Master thesis.
879 Geographisches Institut der Universität Bern (in German).
- 880 Beechie TJ, Pess G, Kennard P, Bilby RE, Bolton S. 2000. Modeling Recovery Rates and
881 Pathways for Woody Debris Recruitment in Northwestern Washington Streams. North
882 American Journal of Fisheries Management 20 : 436–452. DOI: 10.1577/1548-
883 8675(2000)020<0436:mrrapf>2.3.co;2
- 884 Benda LE, Litschert SE, Reeves G, Pabst R. 2016. Thinning and in-stream wood recruitment in
885 riparian second growth forests in coastal Oregon and the use of buffers and tree tipping as
886 mitigation. Journal of Forestry Research 27 : 821–836. DOI: 10.1007/s11676-015-0173-2
- 887 Benda L, Bigelow P. 2014. On the patterns and processes of wood in northern California streams.
888 Geomorphology 209 : 79–97. DOI: 10.1016/j.geomorph.2013.11.028
- 889 Benda L, Miller D, Andras K, Bigelow P, Reeves G, Michael D. 2007. NetMap: A new tool in
890 support of watershed science and resource management. Forest Science 53 : 206–219. DOI:
891 10.1093/forestscience/53.2.206
- 892 Benda LE, Sias JC. 2003. A quantitative framework for evaluating the mass balance of in-stream
893 organic debris. Forest Ecology and Management 172 : 1–16. DOI: 10.1016/S0378-
894 1127(01)00576-X
- 895 Bezzola GR, Gantenbein S, Hollenstein R, Minor HE. 2002. Verklausung von
896 Brückenquerschnitten; Internationales Symposium Moderne Methoden und Konzepte im
897 Wasserbau; Mitteilung der Versuchsanstalt für Wasserbau, Hydrologie und Glaziologie der
898 ETH Zürich, Nr. 175
- 899 [Bishop MP, Giardino JR 2022. Chapter 1.01 - Technology-Driven Geomorphology: Introduction](#)
900 [and Overview. In: Editor\(s\): John \(Jack\) F. Shroder, Treatise on Geomorphology \(Second](#)
901 [Edition\), Academic Press, 2022, Pages 1-17. ISBN 9780128182352, DOI: 10.1016/B978-0-](#)
902 [12-818234-5.00171-1.](#)
- 903 Blaschke T, Tiede D, Heurich M. 2004. 3D landscape metrics to modelling forest structure and
904 diversity based on laser scanning data. International Archives of the Photogrammetry, Remote
905 Sensing and Spatial Information Sciences XXXVI-8W2 : 129–132.
- 906 Bonham-Carter GF, Agterberg FP, Wright DF. 1990. Weights of evidence modelling: a new
907 approach to mapping mineral potential. In Statistical applications in the earth sciences,

- 908 Paper89-9 , Agterberg FP and Bonham-Carter G (eds). Canadian Government Publishing
909 Centre: Ottawa, Ontario, Canada; 171–183.
- 910 Bragg DC. 2000. Simulating catastrophic and individualistic large woody debris recruitment for
911 a small riparian system. *Ecology* 81 : 1383. DOI: 10.2307/177215
- 912 Braudrick CA, Grant GE, Ishikawa Y, Ikeda H. 1997. Dynamics of wood transport in streams: A
913 flume experiment. *Earth Surface Processes and Landforms* 22 : 669–683. DOI:
914 10.1002/(SICI)1096-9837(199707)22:7<669::AID-ESP740>3.3.CO;2-C
- 915 Cavalli M, Trevisani S, Comiti F, Marchi L. 2013. Geomorphometric assessment of spatial
916 sediment connectivity in small Alpine catchments. *Geomorphology* 188 : 31–41. DOI:
917 10.1016/j.geomorph.2012.05.007
- 918 Cislighi A, Rigon E, Lenzi MA, Bischetti GB. 2018. A probabilistic multidimensional approach
919 to quantify large wood recruitment from hillslopes in mountainous-forested catchments.
920 *Geomorphology* 306 : 108–127. DOI: 10.1016/j.geomorph.2018.01.009
- 921 Comiti F, Lucía A, Rickenmann D. 2016. Large wood recruitment and transport during large
922 floods: A review. *Geomorphology* 269: 23–39. DOI: 10.1016/j.geomorph.2016.06.016
- 923 Dixon SJ. 2013. Investigating the effects of large wood and forest management on flood risk and
924 flood hydrology, University of Southampton
- 925 Dorren L. 2017. FINT – Find individual trees. User manual. ecorisQ paper.
- 926 Downs PW, Simon A. 2001. Fluvial geomorphological analysis of the recruitment of large woody
927 debris in the Yalobusha river network, Central Mississippi, USA. *Geomorphology* 37 : 65–91.
928 DOI: 10.1016/S0169-555X(00)00063-5
- 929 Eaton BC, Hassan MA, Davidson SL. 2012. Modeling wood dynamics, jam formation, and
930 sediment storage in a gravel-bed stream. *Journal of Geophysical Research: Earth Surface* 117:
931 1–18. DOI: 10.1029/2012JF002385
- 932 [Finch B, Ruiz-Villanueva V. 2022. Exploring the potential of the Graph Theory to large wood](#)
933 [supply and transfer in river networks. EGU22-8232. DOI: 10.5194/egusphere-egu22-8232](#)
934 [EGU General Assembly 2022.](#)
- 935 FOEN. 2019. Schwemmholz in Fliessgewässern. Ein praxisorientiertes Forschungsprojekt.
936 Bundesamt für Umwelt, Bern. Umwelt-Wissen Nr. 1910, 100 p.
- 937 FOEN. 2015. Einzugsgebietsgliederung Schweiz, EZGG-CH. Bundesamt für Umwelt, Bern.
938 <http://www.bafu.admin.ch/ezgg-ch>

- 939 [Franceschi S, Antonello A, Vela AL, Cavalli M, Crema S, Tonon G, Comiti F.](#) ~~Franceschi S,~~
940 ~~Antonello A, Crema S, Comiti F.~~ 2019. GIS-based approach to assess large wood transport in
941 mountain rivers during floods. Preprint DOI: 10.13140/RG.2.2.31787.08480
- 942 Gasser E, Perona P, Dorren L, Phillips C, Hübl J, Schwarz M. 2020. A new framework to model
943 hydraulic bank erosion considering the effects of roots. *Water (Switzerland)* 12 DOI:
944 10.3390/w12030893
- 945 Gasser E, Schwarz M, Simon A, Perona P, Phillips C, Hübl J, Dorren L. 2019. A review of
946 modeling the effects of vegetation on large wood recruitment processes in mountain
947 catchments. *Earth-Science Reviews* 194 : 350–373. DOI: 10.1016/j.earscirev.2019.04.013
- 948 Gasser E, Simon A, Perona P, Dorren L, Hübl J, Schwarz M. 2018. Quantification of potential
949 recruitment of large woody debris in mountain catchments considering the effects of
950 vegetation on hydraulic and geotechnical bank erosion and shallow landslides. Paquier A and
951 Rivière N (eds). *E3S Web of Conferences* 40 DOI: 10.1051/e3sconf/20184002046
- 952 Ginzler C, Price B, Bösch R, Fischer C, Hobi ML, Psomas A, Rehush N, Wang Z, Waser LT.
953 2019. Area-Wide Products. In *Swiss National Forest Inventory – Methods and Models of the*
954 *Fourth Assessment* , Fischer C and Traub B (eds). Springer International Publishing: Cham;
955 125–142.
- 956 von Glutz M. 2011. Verfahren zur Abschätzung des Schwemholzpotentials von Wildbächen.
957 Bachelor thesis. Schweizerische Hochschule für Landwirtschaft (SHL), Zollikofen,
958 Switzerland. 116 p. (in German)
- 959 Gregory SV, Meleason MA, Sobota DJ. 2003. Modeling the dynamics of wood in streams and
960 rivers. In *American Fisheries Society Symposium* 37 , Gregory S V., Boyer K, and Gurnell A
961 (eds). 315–335.
- 962 [Gurnell AM, Bertoldi W. 2020. Wood in Fluvial Systems. 2nd ed. Elsevier Inc. Editor\(s\): John](#)
963 [\(Jack\) F. Shroder, Treatise on Geomorphology \(Second Edition\), Academic Press, 2022, Pages](#)
964 [320-352, ISBN 9780128182352. DOI: 10.1016/B978-0-12-409548-9.12415-7](#)
- 965 Harmon ME, Franklin JF, Swanson FJ, Sollins P, Gregory SV, Lattin JD, Anderson NH, Cline
966 SP, Aumen NG, Sedell JR, Lienkaemper GW, Cromack K, Cummins KW. 1986. Ecology of
967 coarse woody debris in temperate ecosystems. In: MacFadyen, A.; Ford, E. D., eds. *Advances*
968 *in ecological research*. Orlando, FL: Academic Press, Inc.: 15: 133-302.
- 969 Hassan MA, Bird S, Reid D, Hogan D. 2016. Simulated wood budgets in two mountain streams.
970 *Geomorphology* 259 : 119–133. DOI: 10.1016/j.geomorph.2016.02.010
- 971 Hunziker G. 2017. Schwemholz Zulg. Untersuchungen zum Schwemholzaufkommen in der

- 972 Zulg und deren Seitenbächen. Hunziker Gefahrenmanagement Bericht (Gemeinde
973 Steffisburg).
- 974 Hunzinger L, Durrer S. 2008. Seitenerosion, in: Bezzola, G.R., Hegg, C. (Eds.), Ereignisanalyse
975 Hochwasser 2005, Teil 2 – Analyse von Prozessen, Massnahmen Und Gefahrengrundlagen.
976 Umwelt-Wissen, Nr. 0825, Bundesamt für Umwelt BAFU & Eidg. Forschungsanstalt WSL,
977 Bern, pp. 125-136 (in German).
- 978 Hupp CR, Simon A. 1991. Bank accretion and development of vegetated depositional surfaces
979 along modified alluvial channels, *Geomorphology*, 4, 111-124.
- 980 Kasprak A, Magilligan FJ, Nislow KH, Snyder NP. 2012. A LIDAR-derived evaluation of
981 watershed-scale large woody debris sources and recruitment mechanisms: Coastal Maine,
982 USA. *River Research and Applications* 28 : 1462–1476. DOI: 10.1002/rra.1532
- 983 Kennard P, Pess G, Beechie T, Bilby R, Berg D. 1999. Riparian-in-a-box: A manager’s tool to
984 predict the impacts of riparian management on fish habitat. In *Forest–Fish Conference: Land
985 Management Practices Affecting Aquatic Ecosystems*. Natural Resources Canada, Canadian
986 Forest Service Information Report NOR-X-356. , Brewin M and Monit D (eds). Calgary,
987 Alberta, Canada; 483–490.
- 988 Lassetre NS, Kondolf GM. 2012. Large woody debris in urban stream channels: Redefining the
989 problem. *River Research and Applications* 28 : 1477–1487. DOI: 10.1002/rra.1538
- 990 Losey S, Wehrli A. 2013. Schutzwald in der Schweiz. Vom Projekt SilvaProtect-CH zum
991 harmonisierten Schutzwald . Bern, Schweiz
- 992 Lucía A, Andrea A, Daniela C, Marco C, Stefano C, Silvia F, Enrico M, Martin N, Stefan S,
993 Francesco C. 2015a. Monitoring and Modeling Large Wood Recruitment and Transport in a
994 Mountain Basin of North-Eastern Italy. In *Engineering Geology for Society and Territory -
995 Volume 3*. Springer International Publishing: Cham; 155–158.
- 996 Lucía A, Comiti F, Borga M, Cavalli M, Marchi L. 2015b. Dynamics of large wood during a flash
997 flood in two mountain catchments. *Natural Hazards and Earth System Sciences* 15 : 1741–
998 1755. DOI: 10.5194/nhess-15-1741-2015
- 999 Lucía A, Schwientek M, Eberle J, Zarfl C. 2018. Planform changes and large wood dynamics in
1000 two torrents during a severe flash flood in Braunsbach, Germany 2016. *Science of the Total
1001 Environment* 640–641 : 315–326. DOI: 10.1016/j.scitotenv.2018.05.186
- 1002 Malanson GP, Kupfer JA. 1993. Simulated fate of leaf litter and large woody debris at a riparian
1003 cutbank. *Canadian Journal of Forest Research* 23 : 582–590.

- 1004 Martin D, Benda L. 2001. Patterns of in-stream wood recruitment and transport at the watershed
1005 scale. In Transactions of the American Fisheries Society 130 , . 940–958.
- 1006 [Mazzorana B, Ruiz-Villanueva V, Marchi L, Cavalli M, Gems B, Gschnitzer T, Mao L, Iroumé](#)
1007 [A, Valdebenito G. 2018. Assessing and mitigating large wood-related hazards in mountain](#)
1008 [streams: recent approaches. Journal of Flood Risk Management 11 : 207–222. DOI:](#)
1009 [10.1111/jfr3.12316](#)
- 1010 Mazzorana B, Hübl J, Zischg A, Largiader A. 2011. Modelling woody material transport and
1011 deposition in alpine rivers. Natural Hazards 56 : 425–449. DOI: 10.1007/s11069-009-9492-y
- 1012 Mazzorana B, Zischg A, Largiader A, Hübl J. 2009. Hazard index maps for woody material
1013 recruitment and transport in alpine catchments. Natural Hazards and Earth System Science 9 :
1014 197–209. DOI: 10.5194/nhess-9-197-2009
- 1015 Meleason MA, Gregory S V., Bolte JP. 2003. Implications of riparian management strategies on
1016 wood in streams of the Pacific northwest. Ecological Applications 13 : 1212–1221. DOI:
1017 10.1890/02-5004
- 1018 [Minor KP. 1997. Estimating large woody debris recruitment from adjacent riparian areas, Oregon](#)
1019 [State University, Corvallis, Oregon, USA](#)
- 1020 Montgomery DR, Dietrich WE. 1994. A physically based model for the topographic control on
1021 shallow landsliding. Water Resources Research 30 : 1153–1171. DOI: 10.1029/93WR02979
- 1022 Montgomery DR, Piégay H. 2003. Wood in rivers: interactions with channel morphology and
1023 processes. Geomorphology 51 : 1–5. DOI: 10.1016/S0169-555X(02)00322-7
- 1024 Murphy ML, Koski K V. 1989. Input and Depletion of Woody Debris in Alaska Streams and
1025 Implications for Streamside Management. North American Journal of Fisheries Management
1026 9 : 427–436. DOI: 10.1577/1548-8675(1989)009<0427:iadowd>2.3.co;2
- 1027 [Nakamura F, Seo J Il, Akasaka T, Swanson FJ. 2017. Large wood, sediment, and flow regimes:](#)
1028 [Their interactions and temporal changes caused by human impacts in Japan. Geomorphology](#)
1029 [279: 176–187. DOI: 10.1016/j.geomorph.2016.09.001.](#)
- 1030 Piégay H, Thévenet A, Citterio A. 1999. Input, storage and distribution of large woody debris
1031 along a mountain river continuum, the Drôme River, France. CATENA 35 : 19–39. DOI:
1032 10.1016/S0341-8162(98)00120-9
- 1033 R Core Team. 2019. R: A Language and Environment for Statistical Computing. R Foundation
1034 for Statistical Computing, Vienna, Austria. <https://www.R-project.org/>
- 1035 Rainville RC, Rainville SC, Linder EL. 1986. Riparian silvicultural strategies for fish habitat

- 1036 emphasis. 186–196 pp.
- 1037 Rickenmann D. 1997. Schwemmholz und Hochwasser. *Wasser, Energie, Luft* 89 : 115-119 (in
1038 German).
- 1039 Rickenmann, D., Canuto, N., Koschni, A. 2008. Ereignisanalyse Hochwasser 2005. Teilprojekt
1040 Vertiefung Wildbäche: Einfluss von Lithologie/Geotechnik und Niederschlag auf die
1041 Wildbachaktivität beim Hochwasser 2005. Birmensdorf, Switzerland.
- 1042 Rickenmann, D., Koschni, A. 2010. Sediment loads due to fluvial transport and debris flows
1043 during the 2005 flood events in Switzerland. *Hydrol. Process.* 24, 993–1007.
1044 doi:10.1002/hyp.7536
- 1045 Rickenmann D, Badoux A, Hunzinger L. 2016. Significance of sediment transport processes
1046 during piedmont floods: the 2005 flood events in Switzerland. *Earth Surface Processes and
1047 Landforms* 41 : 224–230. DOI: 10.1002/esp.3835
- 1048 Rickli C, Badoux A, Rickenmann D, Steeb N, Waldner P. 2018. Large wood potential, piece
1049 characteristics, and flood effects in Swiss mountain streams. *Physical Geography* 3646 : 1–23.
1050 DOI: 10.1080/02723646.2018.1456310
- 1051 Rickli, C., Mc Ardell, B., Badoux, A., Loup, B., 2016. Database shallow landslides and hillslope
1052 debris flows, in: Koboltschnig, G. (Ed.), 13th Congress INTERPRAEVENT 2016. 30 May to
1053 2 June 2016. Lucerne, Switzerland. International Research Society INTERPRAEVENT,
1054 Klagenfurt, Austria, pp. 242–243.
- 1055 Rickli C, Bucher H. 2006. Einfluss ufernaher Bestockungen auf das Schwemmholzvorkommen
1056 in Wildbächen . Eidg. Forschungsanstalt für Wald Schnee und Landschaft WSL: Birmensdorf,
1057 94 pp. (in German)
- 1058 Rigon E, Comiti F, Lenzi MA. 2012. Large wood storage in streams of the Eastern Italian Alps
1059 and the relevance of hillslope processes. *Water Resources Research* 48 : 1–18. DOI:
1060 10.1029/2010WR009854
- 1061 Rimböck A. 2001. Luftbildbasierte Abschätzung des Schwemmholzpotentials (LASP) in
1062 Wildbächen. In: Festschrift aus Anlass des 75-jährigen Bestehens der Versuchsanstalt für
1063 Wasserbau und Wasserwirtschaft der Technischen Universität München in Obernach
- 1064 Rimböck A. 2003. Schwemmholzurückhalt in Wildbächen: Grundlagen zu Planung und
1065 Berechnung von Seilnetzsperrern . Ausgabe 94. Lehrstuhl und Versuchsanstalt für Wasserbau
1066 und Wasserwirtschaft der Technischen Universität München
- 1067 Ruiz-Villanueva V, Mazzorana B, Bladé E, Bürkli L, Iribarren-Anacona P, Mao L, Nakamura F,

- 1068 Ravazzolo D, Rickenmann D, Sanz-Ramos M, Stoffel M, Wohl E. 2019. Characterization of
1069 wood-laden flows in rivers. *Earth Surface Processes and Landforms*.
1070 <https://doi.org/https://doi.org/10.1002/esp.4603>
- 1071 Ruiz-Villanueva V, Bladé Castellet E, Díez-Herrero A, Bodoque JM, Sánchez-Juny M. 2014a.
1072 Two-dimensional modelling of large wood transport during flash floods. *Earth Surface*
1073 *Processes and Landforms* 39 : 438–449. DOI: 10.1002/esp.3456
- 1074 Ruiz-Villanueva V, Bladé E, Sánchez-Juny M, Marti-Cardona B, Díez-Herrero A, Bodoque JM.
1075 2014b. Two-dimensional numerical modeling of wood transport. *Journal of Hydroinformatics*
1076 16 : 1077. DOI: 10.2166/hydro.2014.026
- 1077 Ruiz-Villanueva V, Díez-Herrero A, Ballesteros JA, Bodoque JM. 2014c. Potential large woody
1078 debris recruitment due to landslides, bank erosion and floods in mountain basins: a quantitative
1079 estimation approach. *River Research and Applications* 30 : 81–97. DOI: 10.1002/rra.2614
- 1080 Ruiz-Villanueva V, Piégay H, Gurnell AM, Marston RA, Stoffel M. 2016. Recent advances
1081 quantifying the large wood dynamics in river basins: New methods and remaining challenges.
1082 *Reviews of Geophysics* 54 : 611–652. DOI: 10.1002/2015RG000514
- 1083 Ruiz-Villanueva V, Stoffel M. 2018. Application of fuzzy logic to large organic matter
1084 recruitment in forested river basins. *Proceedings of the 5th IAHR Europe Congress —New*
1085 *Challenges in Hydraulic Research and Engineering* : 467–468. DOI: 10.3850/978-981-11-
1086 2731-1_047-cd
- 1087 Ruiz-Villanueva V, Wyzga B, Zawiejska J, Hajdukiewicz M, Stoffel M. 2015. Factors controlling
1088 large-wood transport in a mountain river. *Geomorphology* DOI:
1089 10.1016/j.geomorph.2015.04.004
- 1090 Ruiz-Villanueva V, Bodoque JM, Díez-Herrero A, Eguibar MA, Pardo-Igúzquiza E. 2013.
1091 Reconstruction of a flash flood with large wood transport and its influence on hazard patterns
1092 in an ungauged mountain basin. *Hydrological Processes* 27 : 3424–3437. DOI:
1093 10.1002/hyp.9433
- 1094 Ruiz-Villanueva V, Gamberini C, Bladé E, Stoffel M, Bertoldi W. 2020. Numerical Modeling of
1095 Instream Wood Transport, Deposition, and Accumulation in Braided Morphologies Under
1096 Unsteady Conditions: Sensitivity and High-Resolution Quantitative Model Validation. *Water*
1097 *Resources Research* 56 : 1–22. DOI: 10.1029/2019WR026221
- 1098 Ruiz-Villanueva V, Badoux A, Rickenmann D, Böckli M, Schläfli S, Steeb N, Stoffel M, Rickli
1099 C. 2018. Impacts of a large flood along a mountain river basin: the importance of channel
1100 widening and estimating the large wood budget in the upper Emme River (Switzerland). *Earth*

- 1101 Surface Dynamics, June, 1–42. <https://doi.org/https://doi.org/10.5194/esurf-6-1115-2018>
- 1102 RStudio Team. 2021. RStudio: Integrated Development Environment for R. RStudio, PBC,
1103 Boston, MA URL <http://www.rstudio.com/>
- 1104 Simon A. 1989. Shear-strength determination and stream-bank instabil- ity in loess-derived
1105 alluvium, West Tennessee, USA, in Applied Quaternary Research, edited by E. J. DeMulder
1106 and B. P. Hageman, pp. 129-146, A. A. Balkema Publications, Rotterdam.
- 1107 Schalko I. 2019. Laboratory Flume Experiments on the Formation of Spanwise Large Wood
1108 Accumulations: I. Effect on Backwater Rise Water Resources Research. DOI:
1109 10.1029/2018WR024649
- 1110 Schalko I, Schmocker L, Weitbrecht V, Boes RM. 2018. Backwater Rise due to Large Wood
1111 Accumulations. Journal of Hydraulic Engineering 144 : 04018056. DOI:
1112 10.1061/(ASCE)HY.1943-7900.0001501
- 1113 Schloerke B, Cook D, Larmarange J, Briatte F, Marbach M, Thoen E, Elberg A, Crowley J. 2021.
1114 GGally: Extension to 'ggplot2'. R package version 2.1.2. [https://CRAN.R-](https://CRAN.R-project.org/package=GGally)
1115 [project.org/package=GGally](https://CRAN.R-project.org/package=GGally)
- 1116 Schmocker L, Weitbrecht V. 2013. Driftwood : Risk Analysis and Engineering Measures. Journal
1117 of Hydraulic Engineering 139 : 683–695. DOI: 10.1061/(ASCE)HY.1943-7900.0000728.
- 1118 Seo J, Nakamura F, Chun KW. 2010. Dynamics of large wood at the watershed scale: A
1119 perspective on current research limits and future directions. Landscape and Ecological
1120 Engineering 6 : 271–287. DOI: 10.1007/s11355-010-0106-3
- 1121 Van Sickle J, Gregory S V. 1990. Modeling inputs of large woody debris to streams from falling
1122 trees. Canadian Journal of Forest Research 20 : 1593–1601. DOI: 10.1139/x90-211
- 1123 Spreitzer G, Tunnicliffe J, Friedrich H. 2020. Porosity and volume assessments of large wood
1124 (LW) accumulations. Geomorphology 358 : 107122. DOI: 10.1016/j.geomorph.2020.107122
- 1125 Steeb N, Badoux A, Rickli C, Rickenmann D. 2022. Empirical prediction of large wood transport
1126 during flood events. 11th IHAR International Conference on Fluvial Hydraulics, River Flow
1127 2022. Kingston and Ottawa, November 8-10, 2022.
- 1128 [Steeb N, Rickenmann D, Rickli C, Badoux A. 2021. Large wood event database. EnviDat.](https://www.envidat.ch/dataset/large-wood-event-database)
1129 <https://www.envidat.ch/dataset/large-wood-event-database>
- 1130 Steeb N, Badoux A, Rickli C, Rickenmann D. 2019a. Detailbericht zum Forschungsprojekt
1131 WoodFlow: Empirische Schätzformeln. Birmensdorf

- 1132 Steeb N, Badoux A, Rickli C, Rickenmann D. 2019b. Detailbericht zum Forschungsprojekt
1133 WoodFlow: Empirischer GIS-Ansatz. Birmensdorf
- 1134 Steeb N. 2018. Empirical prediction of large wood transport during flood events. 5th IHAR
1135 Europe Congress. New challenges in Hydraulic Research and Engineering. Trento, Italy.
- 1136 Steeb N, Kuratli B, Rickli C, Badoux A, Rickenmann D. 2017a. GIS-Modellierung des
1137 Schwemmholzpotentials in alpinen Einzugsgebieten. Agenda FAN 2/2017 2 : 9–12.
- 1138 Steeb N, Rickenmann D, Badoux A, Rickli C, Waldner P. 2017b. Large wood recruitment
1139 processes and transported volumes in Swiss mountain streams during the extreme flood of
1140 August 2005. *Geomorphology* 279 : 112–127. DOI:
1141 <https://doi.org/10.1016/j.geomorph.2016.10.011>
- 1142 Steel EA, Richards WH, Kelsley KA. 2003. Wood and wildlife: Benefits of river wood to
1143 terrestrial and aquatic vertebrates. In *The ecology and Management of Wood in World Rivers*.
1144 American Fisheries Society Symposium 37 , Gregory S, Boyer K, and Gurnell A (eds). 235–
1145 247.
- 1146 Strahler AN. 1957. Quantitative analysis of watershed geomorphology. *Eos, Transactions*
1147 *American Geophysical Union* 38 : 913–920. DOI: 10.1029/TR038i006p00913
- 1148 Thevenet A, Citterio A, Piegay H. 1998. A new methodology for the assessment of large woody
1149 debris accumulations on highly modified rivers (example of two French Piedmont rivers).
1150 *Regulated Rivers: Research & Management* 14 : 467–483. DOI: 10.1002/(SICI)1099-
1151 1646(1998110)14:6<467::AID-RRR514>3.0.CO;2-X
- 1152 Uchiogi T, Shima J, Tajima H, Ishikawa Y. 1996. Design Methods for Wood-Debris Entrapment.
1153 279–288 pp.
- 1154 Waldner P et al. 2009. Schwemmholz des Hochwassers 2005. Schlussbericht des WSL-
1155 Teilprojekts Schwemmholz der Ereignisanalyse BAFU/WSL des Hochwassers 2005. .
1156 Birmensdorf, 70 pp. (in German)
- 1157 Welty JJ, Beechie T, Sullivan K, Hyink DM, Bilby RE, Andrus C, Pess G. 2002. Riparian aquatic
1158 interaction simulator (RAIS): A model of riparian forest dynamics for the generation of large
1159 woody debris and shade. *Forest Ecology and Management* 162: 299–318. DOI:
1160 10.1016/S0378-1127(01)00524-2
- 1161 [Wohl E, Kramer N, Ruiz-Villanueva V, Scott DN, Comiti F, Gurnell AM, Piegay H, Lininger](#)
1162 [KB, Jaeger KL, Walters DM, Fausch KD. 2019. The Natural Wood Regime in Rivers.](#)
1163 [BioScience 69 \(4\), 259–273. DOI: 10.1093/biosci/biz013](#)

- 1164 Wohl E, Scott DN. 2016. Wood and sediment storage and dynamics in river corridors. *Earth*
 1165 *Surface Processes and Landforms*: n/a-n/a42, 5-23. DOI: 10.1002/esp.3909
- 1166 Wohl E. 2017. Bridging the gaps: An overview of wood across time and space in diverse rivers.
 1167 *Geomorphology*, 279, 3–26. <https://doi.org/10.1016/j.geomorph.2016.04.014>
- 1168 Wondzell SM, Bisson PA. 2003. Influence of wood on aquatic biodiversity. In *The ecology and*
 1169 *Management of Wood in World Rivers*. American Fisheries Society Symposium 37 , Gregory
 1170 S, Boyer K, and Gurnell A (eds). Bethesda, Maryland; 249–263.
- 1171 WSL. 2016. Schweizerisches Landesforstinventar LFI. Daten der Erhebungen 2004/06 (LFI3)
 1172 und 2009/13 (LFI4). Markus Huber 06.06.2016.
- 1173 Zeh Weissmann H, Könitzer C, Bertiller A. 2009. Strukturen der Fließgewässer in der Schweiz.
 1174 Zustand von Sohle, Ufer und Umland (Ökomorphologie); Ergebnisse der
 1175 ökomorphologischen Kartierung. Umwelt-Zustand Nr. 0926 . Bern
- 1176 Zischg AP, Galatioto N, Deplazes S, Weingartner R, Mazzorana B. 2018. Modelling
 1177 spatiotemporal dynamics of large wood recruitment, transport, and deposition at the river reach
 1178 scale during extreme floods. *Water (Switzerland)* 10 : 1134. DOI: 10.3390/w10091134